People's Democratic Republic of Algeria
Ministry of Higher Education and Scientific Research

University M'Hamed BOUGARA – Boumerdès

Institute of Electrical and Electronic Engineering
Department of Power and Control

Final Year Project Report Presented in Partial Fulfilment of the Requirements of the Degree of

'MASTER'

In **Power Engineering**

Option: Power/Control

Title:

Application of Golden Section Search MPPT control to grid-connected wind turbine driven PMSG

Presented By:

- **Khelifa Ayoub**
- **Ben Haoua Seif Eddine**

Supervisor:

Dr. KHELDOUN Aissa

Co-Supervisor:

Dr. AMMAR Abdelkrim

Registration Number:...../2018

ABSTRACT

This project is intended to design a PMSG based wind energy conversion system. Classical controllers, such as P&O MPPT algorithms are employed to ensure maximum power extraction from wind turbine. Speed of the generator is adjusted to match the wind turbine power- speed characteristics. In this project, a new MPPT algorithm is investigated to maximize the power coefficient Cp. The algorithm is based on Golden Section search principle and expected to be faster than the aforementioned algorithms.

ACKNOWLEDGMENT

First and foremost, we are thankful to Allah, for helping us finish this modest work.

*We would like to express our deep gratitude to our supervisor Dr.**A.kheldoune** and Dr. **A.Ammar** for his support and guidance throughout the study and realization of this project*

We would like to extend our thanks to all our teachers who have done their best to transmit their knowledge.

We extend our thanks to our dear parents who helped us during our studies

DEDICATION

I have great pleasure to dedicate this modest work:

- *Our beloved parents and.*
- *To our families.*
- *My brother* ***Ben Haoua Houdeifa*** *and my uncle Drif Ahmed.*
- *To all our teachers and especially our supervisors.*
- *To all my friends wherever they are,and those who have supported us and helped us specially* ***GHedjatti Karim Eddine***

AYOUB AND SEIF

Table of Contents

List of Figures

List of Tables

List of Acronyms

WT	Wind Turbine
WTG	Wind Turbine Generator
WTGS	Wind Turbine Generation System
VSWT	Variable Speed Wind Turbine
DFIG	Doubly Fed Induction Generator
WFSG	wound field synchronous generator
EG	Electrical Generator
WECS	Wind Energy Conversion System
VAWT	Vertical Axis Wind Turbine
HAWT	Horizontal Axis Wind Turbine
PM	Permanent Magnet
PMSG	Permanent Magnet Synchronous Generator
DD	Direct Driven
MPP	Maximum Power Point
MPPT	Maximum Power Point Tracking
GSS	Golden Section Search
P&O	Perturb and Observe
DC	Direct Current
AC	Alternative Current
PWM	Pulse Width Modulation
IGBT	Isolated Gate Bipolar Transistor
MOSFET	Metalo-Oxcide Semiconductor Field Effect Transistor
CCM	Continuous Conduction Mode
DCM	Discrete Conduction Mode
THD	Total Harmonic Distortion
SVM	Space Vector Modulation
VSC	Voltage Source Control
CSC	Current Source Control
PLL	Phase Locked Loop
VOC	Voltage Oriented Control

General Introduction

The growing demand of the energy around the world and both high cost and exhaustion of the fossil fuels, raised the need to look for alternative sources of energy. Clean, free and endless, renewable energies are the typical replacement for the exhaustible sources. The interest in these sources such as wind, solar and hydraulic energies has grown more and more through the past years, turning it today to one of the biggest industries in the world. Among the several renewable energy sources, wind energy is the most interesting source of energy at present, due to its reliability and low cost it has become the fastest growing power sector in the world and becomes more widely adopted in the future.

Wind energy conversion system (WECS) is what converts that kinetic energy in the wind to the electrical energy using different types and sizes of wind turbines. But since wind speed varies randomly, this will cause the output power by the wind turbine generator to always fluctuate. Fluctuation can cause instability problems, therefore it is not suitable to connect the wind turbines directly to the power system. To overcome such problems the control of the output power from the wind energy generator is needed. This control system will not only eliminate the fluctuation but it will also optimize the output power by tracking its maximum power point (MPP). In order to achieve this, power converters as well as other power electronics are used in addition to several control strategies, such as pitch control, yaw control, and maximum power point tracking (MPPT).

In this report we will discuss and talk about the optimization of the WECS, a novel MPPT technique called the Golden Section Search (GSS) algorithm has been proposed, in order to harvest the maximum power from the wind and inject it into the utility grid. The aim of this work is to model simulate using Matlab/Simulink software a grid tied wind turbine driven a PMSG using the proposed MPPT algorithm. For the simulation several models were needed; the wind turbine mathematical model was developed in addition to the wind turbine's generator model a permanent magnet synchronous generator (PMSG) was used, also blocks for a AC/DC rectifier, a DC/DC converter, DC/AC inverter, a transformer and an AC source representing the power grid. To meet the objective of this project the implementation of this wind energy conversion system was done and tested.

The first chapter of the thesis will give a thorough literature back ground about wind turbines, different types and components, also we will introduce and describe the wind energy conversion system, its working principle as well as power extraction from the wind.

Chapter two is devoted to illustrate and present the mathematical modeling of different parts of our system such as the wind turbine, the generator and the power electronics, in addition to the grid connection and control system.

The third chapter will talk about the theoretical background of the maximum power point tracking and some of its techniques that are used in WECS. Also, it will describe the proposed technique in this work.

Finally, the fourth chapter includes the simulation and implementation, and the discussion of their results.

CHAPTER 1 : Wind Energy Conversion System.

1.1 Introduction:

The utilization of wind as a source of electrical energy has increased dramatically through the past years, as a free clean and renewable energy, it will surely become one of the main energy sources for the world power generation in the future. As fast growing interdisciplinary Field, wind energy conversion technology is continuously developing. In this chapter we are going to explain this technology, and its different configuration, components and principle of working.

1.2 Wind utilization through history:

The utilization of wind energy can be dated back to 5000 B.C. when sail boats were propelled across the river Nile. It was recorded that from 200 B.C. onwards wind was used as an energy source to pump water, grind grain, and drive vehicles and ships in ancient China and Middle East. The earliest windmills recorded were vertical axis mills. These windmills can be described as simple drag devices. They have been used in the Afghan highlands to grind grain since the seventh century BC.

The first details about horizontal axis windmills are found in historical documents from Persia, Tibet and China at about 1000 AD. The first horizontal axis windmill appeared in England around 1150, in France in 1180, in Germany in 1222 and in Denmark in 1259. This fast development was most likely influenced by the Crusaders, taking the knowledge about windmills from Persia to many places in Europe.

In 1891, the Dane Poul LaCour was the first to build a wind turbine that generated electricity. Danish engineers improved the technology during World Wars 1 and 2 and used the technology to overcome energy shortages. The wind turbines by the Danish company F. L. Smidth built in 1941–42 can be considered forerunners of modern wind turbine generators.

The use of wind energy to generate electricity did not gain ground owing to the dominance of steam turbines in electricity generation. The interest in wind energy was renewed in the mid-1970s following the oil crises and increased concerns over resource conservation. Initially, wind energy started to gain popularity in electricity

generation to charge batteries in remote power systems, residential scale power systems, isolated or island power systems, and utility networks.

Owing to special government support schemes in certain countries (e.g.in Denmark) further development in the field of wind energy utilization took place. In USA, along the mountain passes east of San Francisco and northeast of Los Angeles, huge wind farms were installed.

The first of these wind farms consisted mainly of 50 kW wind turbines. Over the years, the typical wind turbine size increased to about 200 kW at the end of the 1980s. Most wind turbines were imported from Denmark. At the end of the 1980s, about 15 000 wind turbines with a capacity of almost 1500 MW where installed in California. It was until the early 1990s when wind projects really took off the ground, primarily driven by the governmental and industrial initiatives. It was also in 1990s there seemed a shift of focus from onshore to offshore development in major wind development countries, especially in Europe.

Offshore wind turbines were first proposed in Germany in 1930s and first installed in Sweden in 1991 and in Denmark in 1992. By July 2010, there were 2.4 GW of offshore wind turbines installed in Europe.

1.3 Wind Energy Conversion System (WECS):

The wind energy conversion system (WECS) is the system that harvest wind energy and transform it into mechanical power through wind turbine and hence use to directly power a machinery or convert it into electrical power. This system main parts are: wind turbine, electrical generator, control system, interconnection apparatus. Figure 1 shows a model of wind energy conversion system.

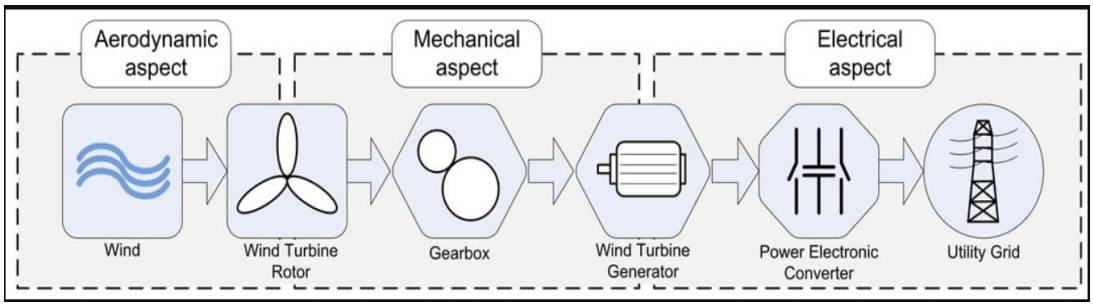

Figure 1.1: Wind energy conversion system model [1].

1.3.1 Wind turbine:

Wind turbines come with different topologies, architectures, size and design features. They are classified based on the structure (horizontal or vertical axis) or on the location (onshore, offshore and deep water), and also based on the control method (constant-speed method, and variable-speed method). But as for the components, modern wind turbines has almost the same parts.as shown in the figure below.

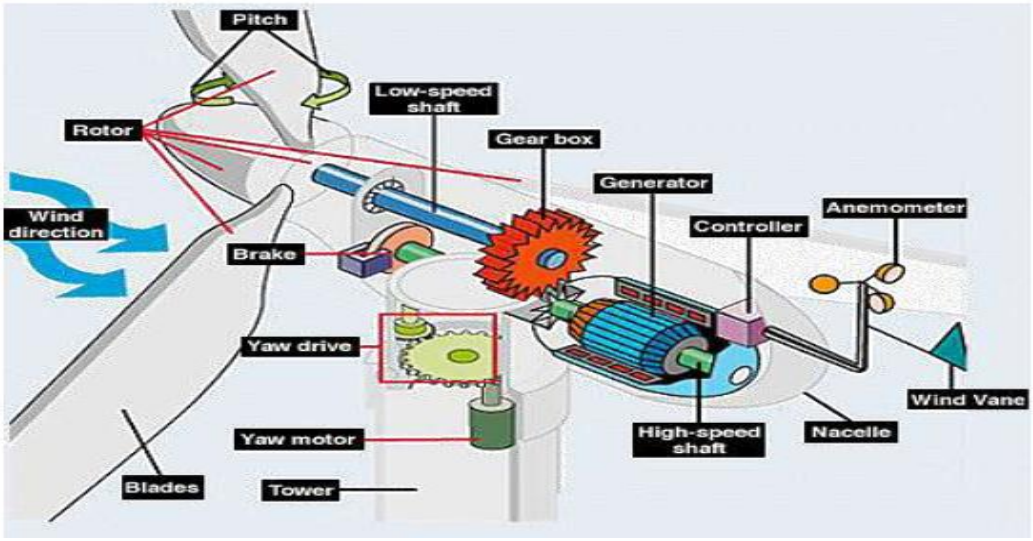

Figure 1.2: Components of the wind turbine [2].

A- Structure of wind turbine:

- **The hub:** it's the component in which the blades are attached to. The hub transfers the motion to the generator inside the nacelle.
- **Rotor blades:** They are the tools that convert the force of the wind into mechanical torque needed to generate useful power. There are many things to consider in designing blades, but most of them fall into one of two categories: Aerodynamics, and Structure.
- **The nacelle:** contains the key components of the wind turbine, including the gearbox, and the electrical generator. It provides weather protection for those components.
- **The tower:** it the base section of the wind turbine that both the nacelle and the rotor are mounted on.

B- Classification of wind turbine:

Horizontal-axis wind turbines (HAWT):

The most common design of modern turbines is based on the horizontal-axis structure. All of the components (blades, shaft, and generator) are on top of a tall tower, and the blades face the wind. In addition to being parallel to the ground, the axis of

blade rotation is parallel to the wind flow. The tower's role is to raise the wind turbine above the ground to intercept stronger winds in order to harness more energy.

The HAWT can be classified as upwind and downwind turbines based on the direction of receiving the wind, in the upwind structure the rotor faces the wind directly, while in downwind structure, the rotor is placed on the lee side of the tower. Figure 2 an example of a horizontal axis wind turbine

Advantages:

• Blades are to the side of the turbines center of gravity, helping stability

• Ability to pitch the rotor blades in a storm to minimize damage

• Tall tower allows placement on uneven land or in offshore locations

Disadvantages:

• Difficult to transport (20% of equipment costs).

• Difficult to install

• Difficult maintenance

Figure 1.3: Horizontal axis wind turbine [3].

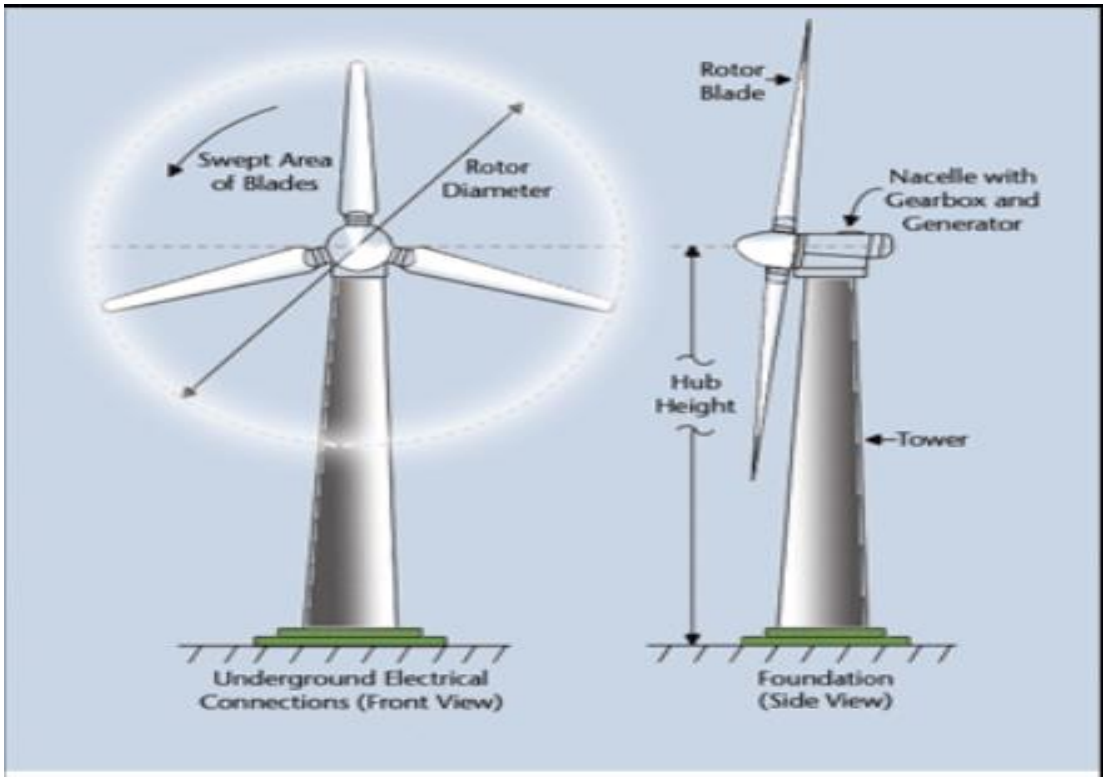

Vertical-axis wind turbine (VAWT):

Vertical axis wind turbines, as shortened to VAWTs, have the main rotor shaft arranged vertically. The vertical axis machine has its blades rotating on an axis perpendicular to the ground. The first windmills were built based on the vertical-axis structure. It is difficult to mount vertical-axis turbines on towers, meaning they are

often installed nearer to the base on which they rest, such as the ground or a building rooftop. The wind speed is slower at a lower altitude, so less wind energy is available for a given size turbine. This type has only been incorporated in small-scale installations.The most common design are the Darrieus, The Savonius and The Giromill turbines. Figure 3 an example of vertical-axis wind turbine

Advantages:

• Easy to maintain

• Lower construction and transportation costs

• Most effective at mesas, hilltops, ridgelines and passes

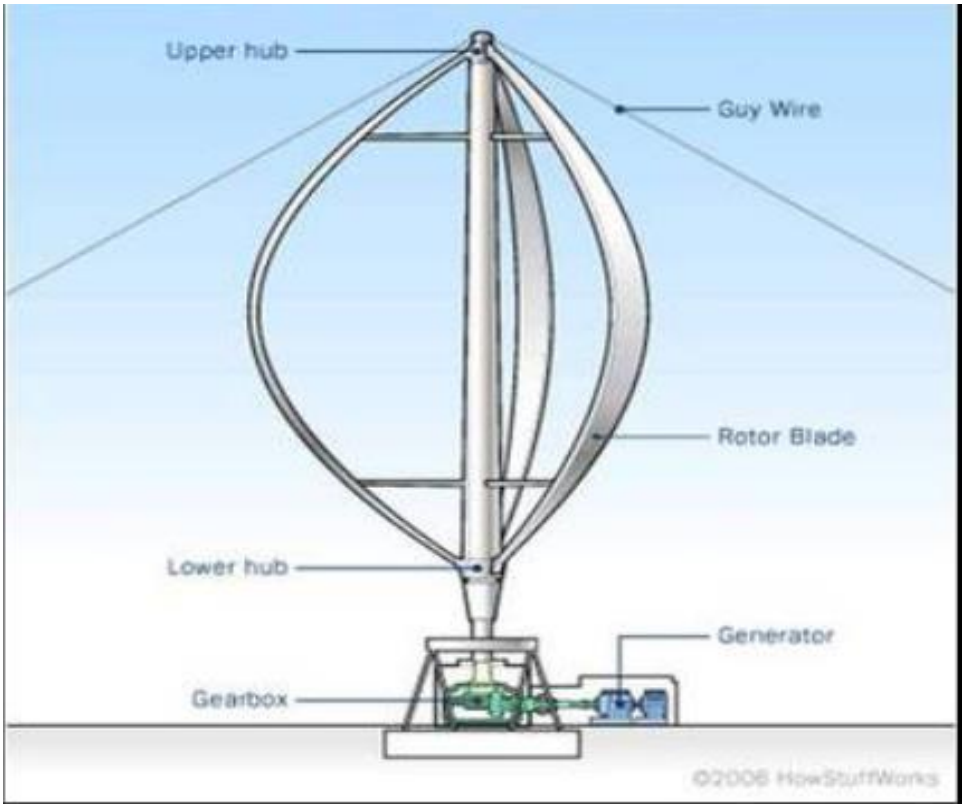

Figure 1.4: Vertical axis wind turbine [4].

Disadvantages:

• Blades constantly spinning back into the wind causing drag

• Less efficient

• Operate in lower, more turbulent wind

1.3.2 Gearbox:

Drive trains in wind energy conversion system commonly includes a gearbox which is used typically in the WT to transform slow speed, high torque of the rotor

blades to the higher speed for the shaft of the electrical generator, since that increase in speed is needed to improve the efficiency of the EG that operates at high speed comparing to wind turbine rotors. Gearbox also used for supporting the heaviest component of the wind turbine.

Gearbox failures are the most occurring faults in the wind energy conversion systemwhich makes it a major drawback in the operation of wind turbines, especially for offshore wind turbines that are situated in harsh and less-accessible environments. Because of this, a new topology has become increasingly adopted in which they remove the gearbox, and connects the wind turbine's rotor directly to the shaft of a multi-poles generator.This configuration is called direct driven systems.

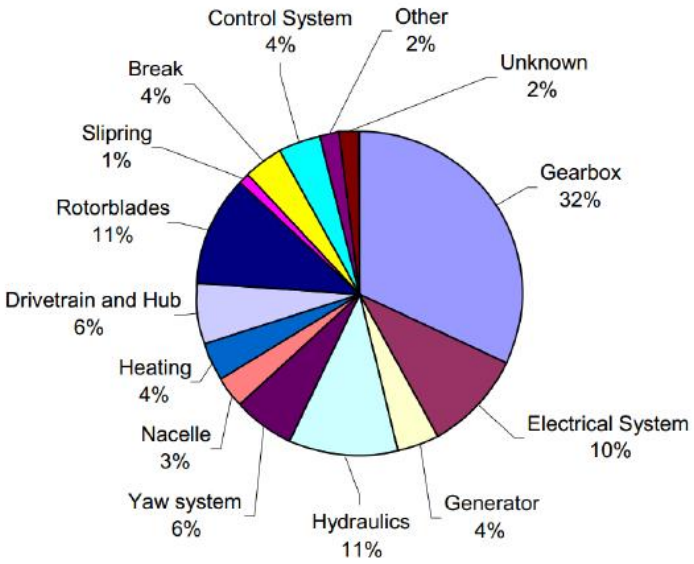

Figure 1.5: Occurring faults in WECS [5].

1.3.3 Electrical Generator [5]:

The generator represents the technical device that allows to convert the mechanical energy extracted from the wind to electrical energy. Modern wind turbines are usually equipped with either an induction generator or a synchronous generator according to the drivetrain system installed. Hereinafter the types of generator commonly engaged in wind turbines technology are listed in the figure below.

Figure 1.6: Types of generator used in WECS [5].

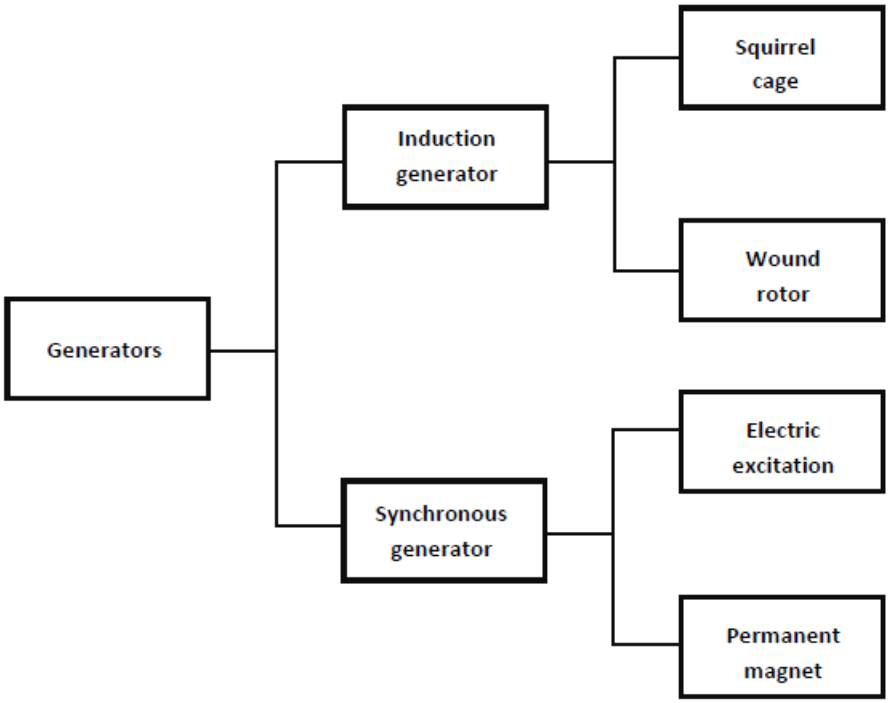

The induction generator is an asynchronous machine which means that rotates asynchronously respect to the magnetic field. With this type of machine the rotor speed varies according to the load applied on the shaft, more is the load higher is the rotor speed, and if any load is applied the generator rounds at synchronous speed. As shown in the figure above, the induction generators can be classified into two categories, respectively: wound rotor and squirrel cage. Both generator types are commonly used for indirect drive wind turbine, therefore they require limited space inside nacelle as well as limited power electronic.

On the contrary, for synchronous generators, the rotor speed is unique and it is of the magnetic field, namely the synchronous speed. In wind turbine industry, two configurations are commonly used, specifically electric excitation and permanent magnet (PM).

The first model is basically installed in small turbines, instead permanent magnet is mostly designed for direct drive wind turbines. PM generators, for direct drive technology, present large sizes because they needs a several numbers of pair poles in order to round at same speed of the rotor blade (e.g. max 15 rpm), so they require large space inside nacelle and also additional space for the cooling system of the power electronic.

1.4 Wind Energy Conversion System Operation:

A wind turbine obtains its power input by converting some of the kinetic energy in the wind into torque acting on the rotor blades. The amount of energy which the WT can harvest from the wind and depends on the wind speed, the blades swept area, blade design (pitch angle) and the density of the air. Although there are many different configurations of wind turbines systems they all work in a similar way .The turbine starts to produce energy when the wind speed is above Vcut-in (typically between 3-5 m/s), and it reaches a maximum speed at the optimal wind speed (typically 12 m/s) and stops when the wind speed exceeds Vcut-off (typically between 22-25 m/s).

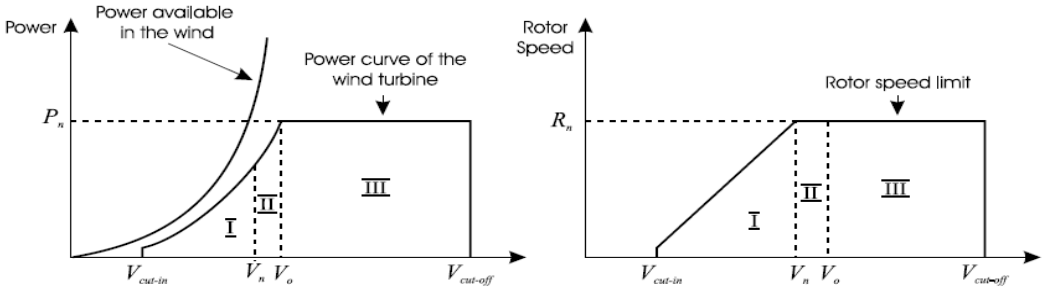

Figure 1.7: Operation regions of wind turbine [6].

1.4.1 Fixed Speed Operation:

A fixed speed WTGS consists of a conventional, directly grid coupled squirrel cage induction generator, which has some superior characteristics such as brushless and rugged construction, low cost, maintenance free, and operational simplicity. The slip and hence the rotor speed of a squirrel cage induction generator varies with the amount of power generated. These rotor speed variations are, however, very small, approximately 1 to 2 % of the rated speed. Therefore, this type of wind energy conversion system is normally referred to as a constant or fixed speed WTGS. The advantage of a constant speed system is that it is relatively simple.

Therefore, the list price of constant speed turbines tends to be lower than that of variable speed turbines. However, constant speed turbines must be more mechanically robust than variable speed turbines. Because the rotor speed cannot be varied, fluctuations in wind speed translate directly into drive train torque fluctuations, causing higher structural loads than with variable speed operation. This partly cancels

the cost reduction achieved by using a relatively cheap generating system. The fixed speed WTGS topology is shown in Figure below.

Figure 1.8: Fixed speed WECS configuration [7].

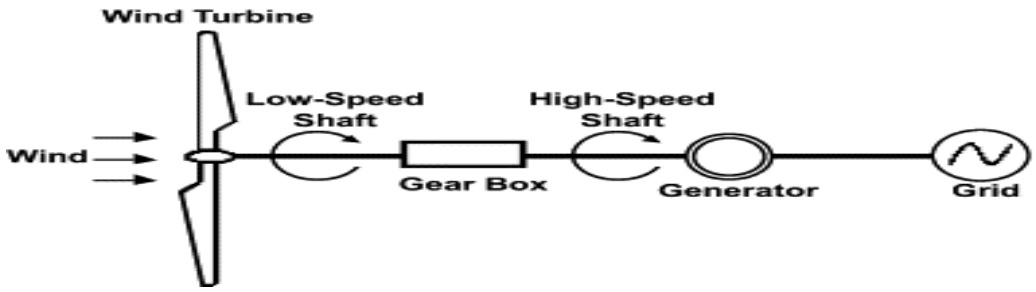

1.4.2 Variable Speed Operation:

Another commercial trend of a wind power generation is in using variable speed wind turbine (VSWT) driving a doubly fed induction generator (DFIG), wound field synchronous generator (WFSG) or permanent magnet synchronous generator (PMSG). The main advantage of variable speed operation is that more energy can be generated for a specific wind speed regime. Although the electrical efficiency decreases due to the losses in the power electronic converters that are essential for variable speed operation, the aerodynamic efficiency increases due to variable speed operation. The aerodynamic efficiency gain can exceed the electrical efficiency loss, resulting in a higher overall efficiency. In addition, the mechanical stress is less because the rotor acts as a flywheel (storing energy temporarily as a buffer), reducing the drive train torque variations. Noise problems are reduced as well because the turbine runs at low speed. The main drawback of variable speed generating systems is that they are more expensive. However, using a variable speed generating system can also give major savings in other subsystems of the turbine such as lighter foundations in offshore applications, limiting the overall cost increase.The currently available variable speed wind turbine generator system topologies are shown in Figure below.

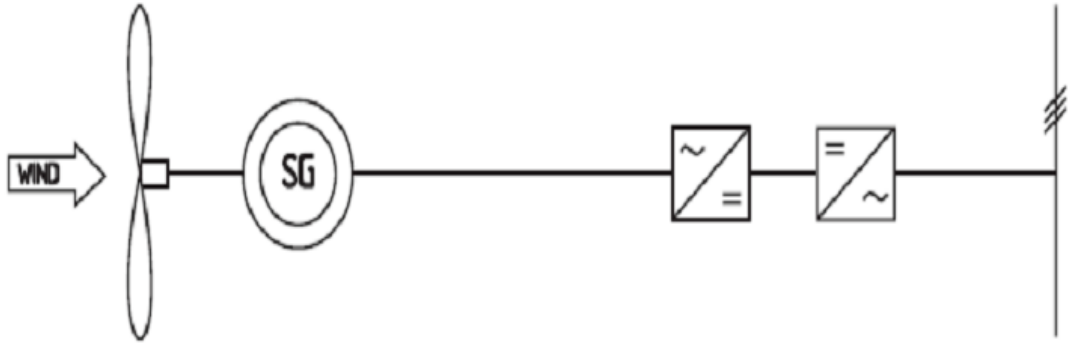

Figure 1.9: Variable speed configuration of direct driven WECS [8].

1.5 Power Extraction in WECS:

The kinetic energy of the wind (air mass m, wind speed v) is given by the following equation:

$$E_c = \frac{1}{2}mv^2 \quad (1.1)$$

With: $m = \rho v S \Delta t$

Where S: Covered surface of the turbine.

ρ: The air density is considered $\rho = 1.08\ kg/m^3$ in this report.

The wind power, P_w has the following expression:

$$P_w = \frac{d}{dt}E = \frac{1}{2}\rho S v^3 \quad (1.2)$$

The mechanical power that the turbine extracts from the wind, P_m, is inferior to P_w because the wind speed after the turbine isn't zero (the air needs to be carried-off after the turbine). So, the power coefficient of the turbine $C_p$can be defined by:

$$\boldsymbol{C_p = \frac{P_m}{P_w}} \quad \text{With} \quad \mathbf{C_p < 1}$$

The recuperated power is given by:

$$P_m = \frac{1}{2}\rho \pi R^2 v^3 C_p \quad (1.3)$$

Where R: radius of the rotor.

Cp is called the power coefficient of the rotor or the rotor efficiency. It is the fraction of the upstream wind power, which is captured by the rotor blades and has a theoretical maximum value of 0.59, shown in Figure. In practical designs, maximum achievable Cp is between 0.4 and 0.5.

It is useful to mention that the output power of a turbine is determined by the effective area of the rotor blades (A), wind speed (v), and wind flow conditions at the rotor (Cp). Thus, the output power of the turbine can be varied by changing the

effective area and/or by changing the flow conditions at the rotor system. Control of these quantities forms the basis of control of wind energy systems.

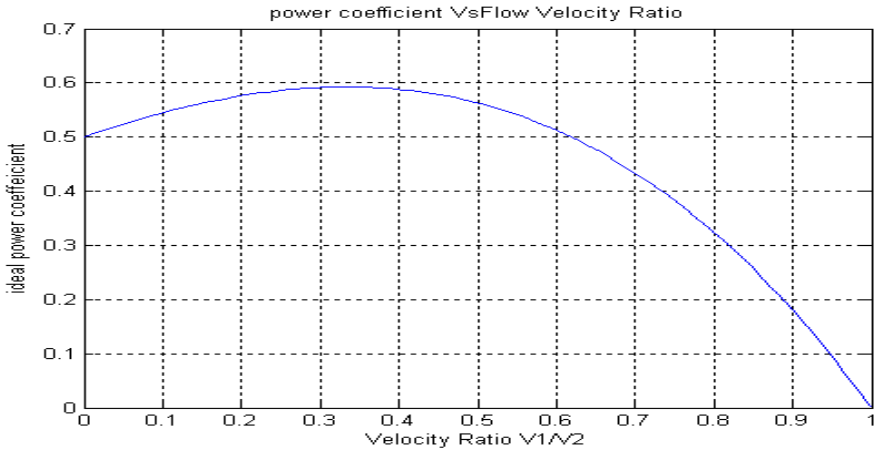

Figure 1.10: Power coefficient as a function of the wind stream ratio [9].

This was first derived by A. Betz, and it has limit called the "Betz factor" or "Betz limit" [9]. This value is the maximum theoretical value of the power coefficient and thus it is also the maximum theoretical efficiency that a wind energy converter can have which is equal to 59.3%. However, this value of the power coefficient was obtained for an ideal, frictionless flow turbine. Therefore, the wind turbine will always have a smaller maximum power coefficient than the Betz factor in practice, because of the various aerodynamic losses that depend on the rotor design and construction (number of blades, weight, stiffness, etc.).

The difference between the power coefficient and the efficiency of a wind turbine system is that the efficiency of a wind turbine includes the loss in the mechanical transmission, electrical generation, converter loss, etc., whereas the power coefficient is the efficiency of converting the power in the wind into mechanical energy in the rotor shaft.

The power coefficient is usually given as a function of the tip speed ratio λ and the blade pitch angle β. The pitch angle is the angle between the plane of rotation and the blade cross-section chord [9]. The tip speed ratio of a wind turbine is defined

$$\lambda = \frac{u}{v_1} = \frac{r\omega}{v_1} = \frac{tangential\ velocity\ of\ the\ rotor\ blade\ tip}{speed\ of\ wind}$$

Where u is the tangential velocity of the blade pitch, ω is the angular velocity of the rotor,

r Is the rotor radius in meters, and υ_1 is the wind speed.

The output power of the wind turbine P_t may be calculated as**:**

$$P_t = \frac{1}{2} C_p(\lambda) \rho A v_w^3 \qquad (1.4)$$

The torque developed by the wind turbine can be expressed as:

$$t_t = \frac{P_t}{\omega} \tag{1.5}$$

Combining equations (1.3), (1.4) and (1.5), the expression for the torque may be written as:

$$t_t = \frac{1}{2}\rho A r \frac{C_p(\lambda)}{\lambda} v^2 \tag{1.6}$$

1.6 Conclusion:

In this chapter we presented the wind energy conversion system, by giving a thorough definition for each of its components. We also discussed the different types of WECS operations. Moreover, a detailed description of the wind turbines based on their types and principle of working has been reported. Finally, we explained the power extraction from the wind using the WTG setting the ground for the next chapter that discusses the dynamic model of our WTG system.

CHAPTER 2 : Modelling of WECS.

2.1 Introduction:

Wind energy conversion systems (WECS) is a vital topic in the whole process of wind energy harvesting. It involve many fields of various disciplines such as kinematics, mechanics, aerodynamics, meteorology, power electronics, power systems, as well as topics covered by structural and civil engineering. The main focus of this chapter is the theoretical background on electrical power interfaces and grid-connected topologies for WECS of this project.

2.2 Rotor Power Characteristics:

The mechanical power that is captured by the wind turbine is given by the following nonlinear equation:

$$P_R = \frac{1}{2}\rho\pi R^2 v_w^3 C_p(\lambda, \beta) \tag{2.1}$$

Where R is the radius of the swept area of the turbine blades, ρ is the wind density and C_p is the power coefficient of the wind turbine and represents the percentage of energy in the wind transformed into mechanical energy in the rotor axis. Note that this coefficient depends on two variables: the ratio of tip speed (λ) and the angle of attack (β). For the purposes of this analysis is considered an angle of attack equal to zero (β = 0) [15]. C_p is given by:

$$C_p(\lambda, \beta) = C_1(C_2\frac{1}{\Lambda} - C_3\beta - C_4\beta^x - C_5)e^{-C_6\frac{1}{\Lambda}} \tag{2.2}$$

The coefficients C_1 to C_6 and X can be different for various turbines. They depend on the wind turbine rotor and blade design. The parameter $\frac{1}{\Lambda}$ is defined as:

$$\frac{1}{\Lambda} = \frac{1}{\lambda+0.08\beta} - \frac{0.035}{1+\beta^3} \tag{2.3}$$

Where the coefficient depends only of the index of tip speed, which is calculated as:

$$\lambda = \frac{w_r}{v} \tag{2.4}$$

For simulation the following values have been chosen for coefficients C_1 to C_6 [16]: C_1=0.043, C2= -0.108, C_3=0.146, C4= -0.062, C_5= -0.0006.

From equation (2.1) the mechanical power extracted from the wind is a function of the wind speed and the power coefficient .If the wind speed is assumed to be constant, then the mechanical power only becomes a function of the power coefficient. The mechanical power can then be expressed as follows:

$$P_R = C_p P_o \tag{2.5}$$

Assuming the wind speed and the blade pitch angle are constant, then the power coefficient becomes a function of the rotor speed ω_R.Therefore the mechanical power can be expressed as:

$$P_R(\omega_R) = C_p(\omega_R)P_o \tag{2.6}$$

Figure 2.1 shows the mechanical power versus the generator rotor speed for different wind speeds. The power coefficient of each turbine will be determined by their blade design and pitch angle (see figure 2.2).

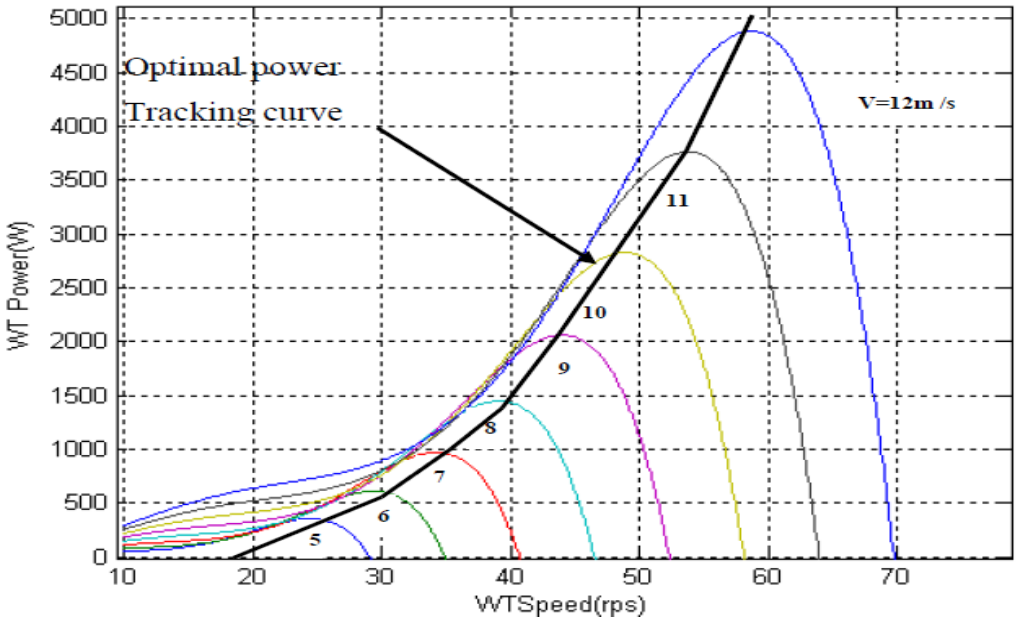

Figure 2-1: Typical power versus speed characteristics of a wind turbine [14].

The power extracted from the wind is maximized when C_p is maximized. This optimal value of C_p occurs at a defined value of the tip speed ratio λ. For each wind speed there is an optimum rotor speed where maximum power is extracted from the wind. Therefore, if the wind speed is assumed to be constant the value of $C_p$depends on the wind turbine rotor speed .Thus, controlling the rotor speed controls the power output of the turbine.

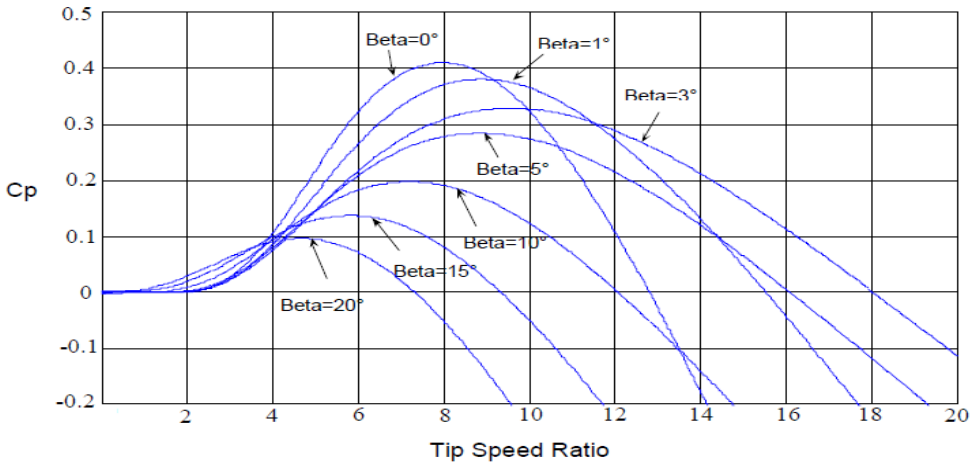

Figure 2-2: Cp-λ characteristics of wind turbines for different values of pitch angle [14].

2.3 The drive train modelling:

The power associated with the wind is transmitted to the electrical generator by a mechanical shaft called "Drive train". The mathematical model of the direct drive train depends on the structure of the wind energy conversion system (WECS) and its power rate. The two-mass drive train system is more suitable for transient stability analysis and has a stronger impact on wind turbine and yields more accurate results during the fluctuation wind conditions [17]. Figure 2.3 displays the two-mass drive train model.

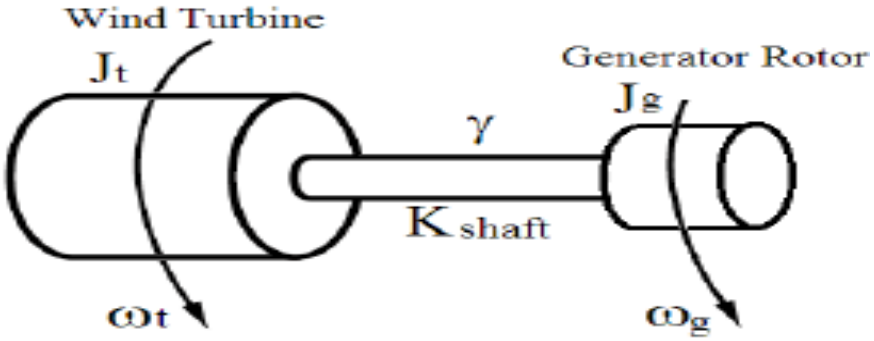

Figure 2-3: Two-mass drive train model [22].

The drive train model considered in this work can be represented by:

$$T_m = \frac{P_m}{w_m} \tag{2.7}$$

$$2H_t \frac{dw_t}{dt} = T_m - T_{sh} \tag{2.8}$$

$$\frac{1}{w_{eb}} \frac{d\theta_{tw}}{dt} = w_t - w_r \tag{2.9}$$

$$T_{sh} = K_{sh}\theta_{tw} + D_t \frac{d\theta_{tw}}{dt} \tag{2.10}$$

Where T_m is the input torque of the generator, P_m is the mechanical power, w_m is the rotor speed, H_t is the turbine inertia, $\theta_{t\omega}$ is the shaft twist angle, ω_t is the turbine rotational speed, ω_r is the generator rotational speed, ω_{elb} is the base electrical speed, T_{sh} is the shaft torque, K_{sh} is the shaft stiffness, and D_t is the damping coefficient. In the case of direct drive train, since there is no gear box, the rotor of the turbine is directly connected to the generator's shaft, which means they have the same speed i.e. $w_t = w_m$.

2.4 Permanent Magnet Synchronous Generator (PMSG):

This type of machine can be used in both fixed and variable speed applications. The PMSG is very efficient and suitable for wind turbine applications.

PMSGs has a lot of advantages that made them more popular in WECS than other generators. Some of these advantages are mentioned here starting from the fact that the PMSGs have a high reliability (i.e. PMSGs have a less failure ratio) due to the fact that they are brushless and without slip rings, the existence of brushes and slip rings in generators requires additional maintenance which is avoided when using PMSGs. Furthermore the PMSGs don't need excitation, thus; a reduction in power electronics circuits in WECS. Finally, PMSGs allow direct-drive (DD) energy conversion for wind applications. DD energy conversion helps eliminate the gearbox between the turbine and generator; thus these systems are less expensive and require less maintenance [13]. However, the lower speed determined by the turbine shaft is the operating speed for the generator.

2.4.1 The dynamic model of the PMSG:

To simplify the analysis, The PMSG is normally modelled in the rotor field (dq-axis) synchronous reference Frame, which the q-axis is 90° ahead of the d-axis with respect to the direction of rotation. The rotor has two axes which the axis that is aligned with the rotor and flux is called d-axis and the perpendicular axis to d-axis called q-axis The flux caused by PM is in the direction of d-axis, the angle between stator axis and d-axis is called Θe as shown in figure 2.4.

The synchronization between the d-q rotating reference frame and the abc-three phase frame is maintained by utilizing a phase locked loop. The voltage equations for the synchronous generator are given by:

$$V_{ds} = -R_s i_{ds} - w_{gr}\lambda_{qs} + p\lambda_{ds} \quad (2.11)$$

And

$$V_{qs} = -R_s i_{qs} - w_{gr}\lambda_{ds} + p\lambda_{qs} \quad (2.12)$$

Where

$$\lambda_{ds} = -L_d i_{ds} + \lambda_r \quad (2.13)$$

$$\lambda_{qs} = -L_q i_{qs} \quad (2.14)$$

Where λr is the rotor flux which is constant in the PMSG so, $d\lambda r/dt$=0, L_d and L_q are the stator dq-axis self-inductances.

Substitute from equations (2.13) and (2.14) in (2.11) and (2.12) yield:

$$V_{ds} = -R_s + w_{gr}L_q i_{qs} - pL_d i_{ds} \quad (2.15)$$

$$V_{qs} = -R_s i_{qs} - w_{gr}L_d i_{ds} + w_{gr}\lambda_r - pL_q i_{qs} \quad (2.16)$$

D-q-axis model of the PMSG in the rotor-field synchronous reference frame is shown in figure 2.5.

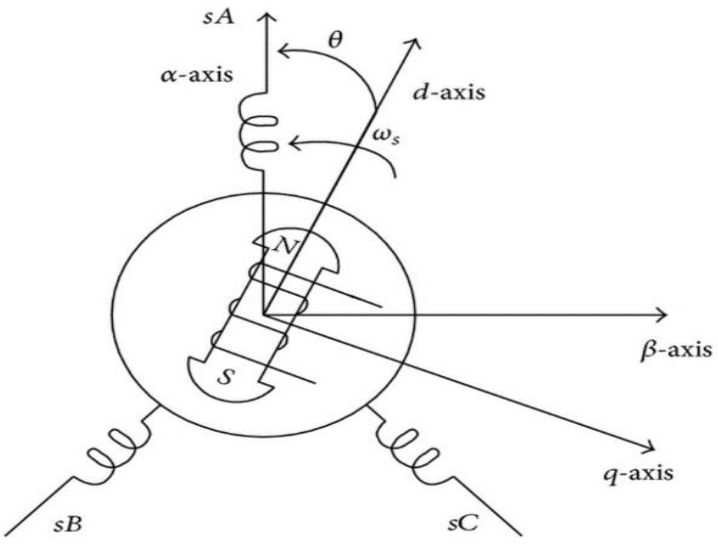

Figure 2-4: The Configuration of the Winding and PM in the PMSG [23].

The PMSG electromagnetic torque is given:

$$T_e = \frac{3p}{2}(i_{qs}\lambda_r - (L_d - L_q)i_{ds}i_{qs}) \quad (2.17)$$

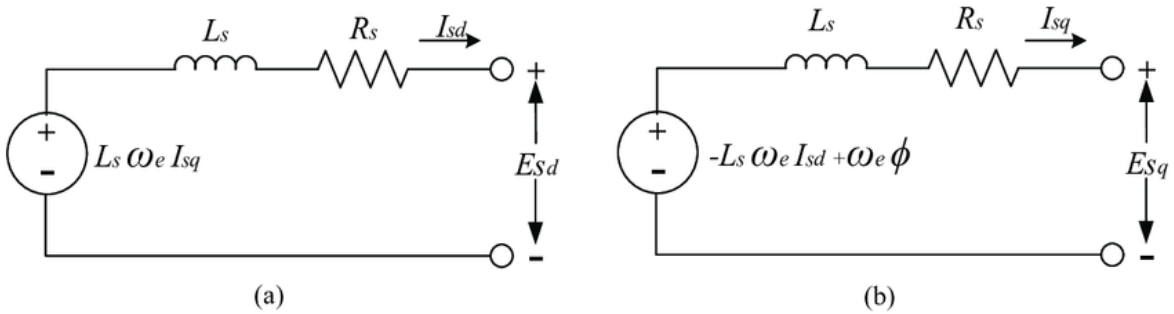

Figure 2-5: Equivalent circuit in (a) D-axis and (b) Q-axis [24].

2.5 Power electronics converters:

The power electronics converters which are selected in this project consist of diode rectifier in order to convert the ac power to dc, a boost type dc-dc converter which is used to control the PMSG , and inverter served as the grid interface (see figure 2.6).[18,19]

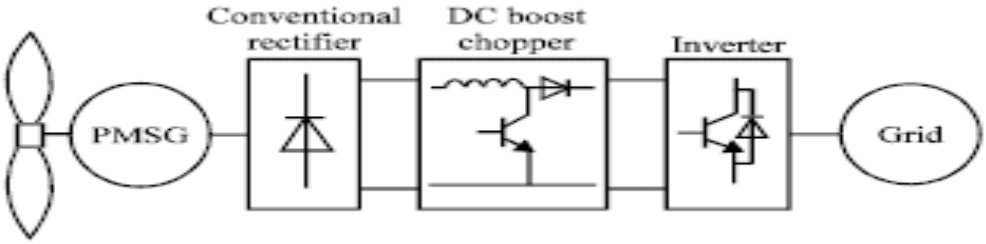

Figure 2-6: Wind energy conversion system scheme [25].

2.5.1 AC to DC diode bridge rectifier:

The diode rectifier converts the three-phase AC voltage of the PMSG into DC voltage, it is the most common used topology in power electronic applications. For a three-phase system it consists of six diodes as shown in figure 2.7.

2.5.1.1 Performance:

The phase voltages va, vb, and vc are equal to:

$v_a = V_m \sin(\omega t)$; $v_b = V_m \sin(\omega t - 120°)$; $v_c = V_m \sin(\omega t - 240°)$

Where Vm is the peak value.

The line to line voltages vab, vbc, and vca are equal to:

$v_{ab} = \sqrt{3}V_m \sin(\omega t + 30)$; $v_{bc} = \sqrt{3}V_m \sin(\omega t - 90)$; $v_{ca} = \sqrt{3}V_m \sin(\omega t - 210)$

The average output voltage is given by the formula:

$$V_{dc} = \frac{6}{2\pi} \int_{\pi/3}^{2\pi/3} \sqrt{3}\, V_m \sin(wt)\, dwt = \frac{3\sqrt{3}}{\pi} V_m \qquad (2.18)$$

The rms output voltage is equal to:

$$V_{rms} = [\frac{9}{\pi} \int_{\pi/3}^{2\pi/3} (V_m \sin(wt))^2\, dwt]^{1/2} = [\frac{3}{2} + \frac{9\sqrt{3}}{4\pi}]^{1/2}\, 1.6554 V_m \qquad (2.19)$$

If we consider that the load is purl resistive, so the rms value of the diode current is equal to:

$$I_r = [\frac{4}{2\pi}\int_0^{\pi/6} {I_m}^2 \cos wt^2\, dwt]^{1/2} = I_m[\frac{1}{\pi}(\frac{\pi}{6} + \frac{1}{2}\sin\frac{2\pi}{6})]^{1/2} \qquad (2.20)$$

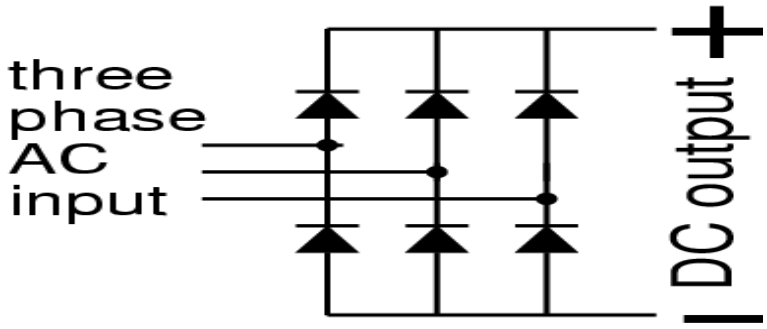

Figure 2-7: 3-phase diode rectifier scheme [26].

2.5.2 DC to DC boost converter:

The boost converter can be used as switching-mode regulator to convert the rectified DC voltage, normally unregulated, to a regulated DC and desired magnitude output voltage used by the followed inverter [20]. The regulation is normally achieved by PWM at a fixed frequency and the switching device is normally IGBT or MOSFET.

Figure 2.8 illustrates a boost converter, which consists of a voltage source V_{dc1}, an inductor L_{dc}, which is used for energy storage and connected to the voltage source in series, a switching device SW, a diode, a filter capacitor C_{dc} and a load with output voltage V_{dc}. In this model, the boost converter has been controlled to yield constant output DC voltage level, V_{dc2} by varying the duty ratio, D in response to variations in V_{dc1}.

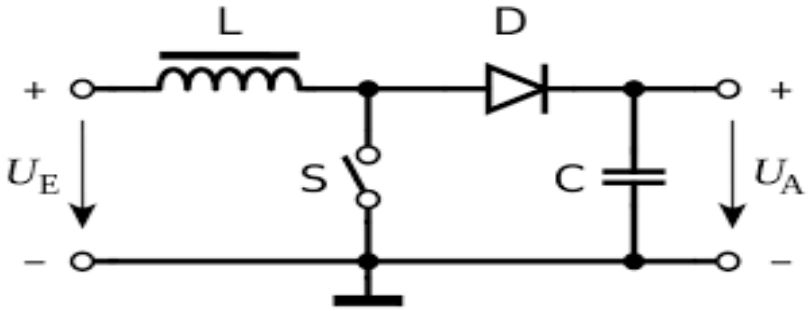

Figure 2-8: Boost converter scheme [27].

Mode of operation:

From the previous figure the energy from the voltage source is stored in the inductor L_{dc} when the switching device SW is conducting. The current through the

inductor increases linearly, the diode is reverse biased and the capacitor provides voltage for the load during that time. When the switching device SW is opened, the diode conducting the current through the inductor L_{dc}, and diode Doffers power for the load and the charging of the capacitor C_{dc}. The relation between the input and output voltage and currents of the boost converter for a given period T and duty ration D is expressed by the following equations:

$$V_{dc1}DT = (V_{dc1} - V_{dc2})(1 - D)T \quad ; \quad V_{dc2} = \frac{1}{(1-D)}V_{dc1} \qquad (2.21)$$

$$I_{dc2} = (1 - D)I_{dc1} \qquad (2.22)$$

It is possible that boost chopper circuit and load resistance R_L are considered a kind of variable resistance changed by duty ratio from the viewpoint of the DC voltage source. This variable resistance R_{dc1} is defined as:

$$R_{dc1} = \frac{V_{dc1}}{I_{dc1}} \qquad (2.23)$$

The output current I_{dc2} is expressed by output voltage V_{dc2} and load resistanceR_L:

$$I_{dc2} = \frac{V_{dc2}}{R_L} \qquad (2.24)$$

By dividing (2.21) by (2.22) we obtain:

$$\frac{V_{dc1}}{I_{dc1}} = \frac{V_{dc2}}{I_{dc2}} \times \frac{1}{(1-D)^2} \qquad (2.25)$$

By dividing (2.23) by (2.24) we obtain:

$$R_{dc1} = (1 - D)^2 R_L \qquad (2.26)$$

From equation (2.23), it was confirmed that the boost chopper from the viewpoint of the DC voltage source could be expressed in the function of the duty ratio.

Once the switching frequency is confirmed, the inductance of L determines the operating mode of the circuit, as given by:

$$L_c = \frac{(1-D)^2 D R_L}{2f} \quad (2.27)$$

Where L_c is the critical value of the inductance and f is the switching frequency, if the inductance Lin the boost converter is greater than L_c, the converter operates in the state of CCM, otherwise it operates in the state of DCM.

2.5.3 DC to AC inverter:

The DC to AC inverter is used to convert the DC output quantities of boost converter to an equivalent AC with a fixed frequency and voltage that it will transferred to utility. A three phase inverter is used for this project instead of single phase since we deal with high-power applications. Figure 2.9 illustrates a common topology of inverter, which consists of an upper bridge (S1, S3, S5) and a lower bridge (S4, S6, S2) there each switch is no more than IGBT. Each of the IGBT pairs in the upper and lower bridges cannot be conducting at the same time, otherwise the power input will be shorted. Therefore the switching state of the upper bridge has to be opposite to that of the lower bridge. [21]

To focus on the upper bridge S1, S3 and S5, if logic '1' indicates the switched on state, and '0' represents switched off state, the three switches have eight state combinations as listed in Table 2-1. In order to reduce the switching times of the IGBT pair in the inverter and to reduce the effects of harmonics, the switching state of IGBT pairs are only changed once within a pulse period.

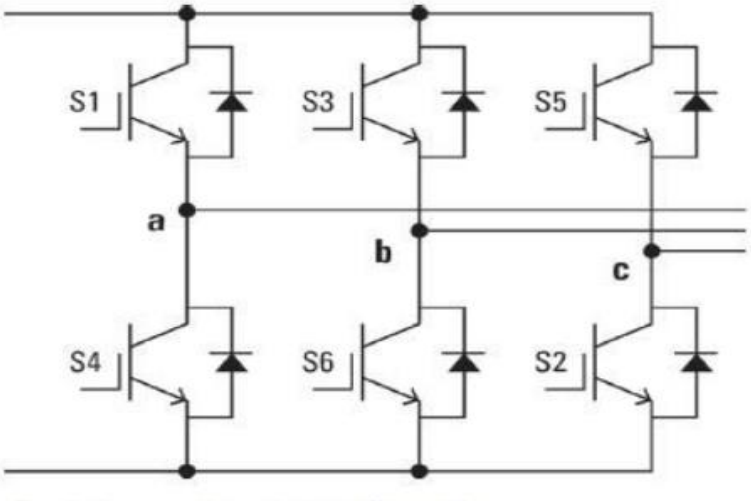

Figure 2-9: DC/AC two level inverter scheme [28].

Table 2-1: The relationship between work mode and phase voltage.

Vector	S5	S3	S1	Va	Vb	Vc
V0	0	0	0	0	0	0
V1	0	0	1	2Vdc/3	-Vdc/3	-Vdc/3
V2	0	1	1	Vdc/3	Vdc/3	-2Vdc/3
V3	0	1	0	-Vdc/3	2Vdc/3	-Vdc/3
V4	1	1	0	-2Vdc/3	Vdc/3	Vdc/3
V5	1	0	0	-Vdc/3	-Vdc/3	2Vdc/3
V6	1	0	1	Vdc/3	-2Vdc/3	Vdc/3
V7	1	1	1	0	0	0

Table 2-1 illustrates that a 3-phase AC power can be synthesized by eight vectors, in which there are two zero vectors V0and V7. A period of the output voltage is divided into 6 patterns, the patterns show the switching state of the upper bridge IGBTs, where lower bridge are just opposite to the upper bridge.

2.5.4 Grid connection:

When a considerable part of the electrical power is coming from the wind turbines, the network operators will have many technical and economical problems to manage the system. Therefore it is clear that one of the important aspects of research must be concentrated on the grid interaction of the wind turbines. One of the main concerns of the network operators is the power quality which depends on what kind of sources are connected to the grid. The wind energy has to be grid compatible, because in any power system the operator has to control the frequency and the voltage. These are the most important grid connection requirements [29].
The scheme of the plant which represents the connection of the wind turbine to the grid starting from the grid side converter as shown in figure 2.10.

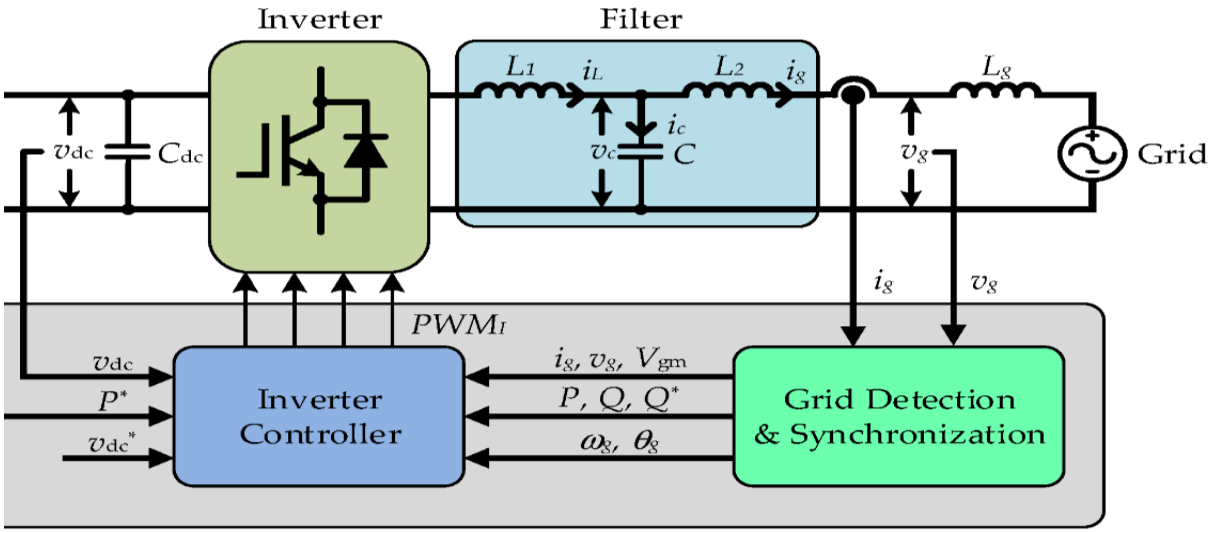

Figure 2-10: Grid connection scheme [30].

The major parts that are considered in the grid connection system of this project are: the filter and the grid side converter control.

2.5.4.1 Filter:

The filter role in the system is to lower the currents total harmonics distortion (THD) since the obtained signal from the inverter contains ripple caused by switching.

The most common types of filters used in grid connection are the L-filter and the LCL-filter, the chosen filter for this project is the L-filter due to its simplicity. The L-filter will be represented by an inductance and a small resistance which takes into account the losses of the inductance. The filter is shown in figure 2.11.

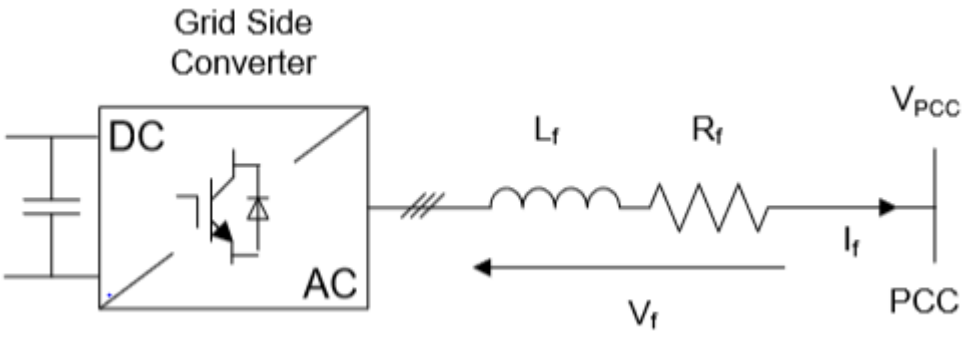

Figure 2-11: DC/AC inverter connected to an L-filter [29].

The transfer function of the L-filter's output current has the following expression:

$$H_f(s) = \frac{I_f(s)}{V_f(s)} = \frac{1}{sL_f + R_f} \qquad (2.28)$$

2.5.4.2 Grid side converter control:

The grid side converter control is an important issue for the grid connection system since it makes sure that the delivered power to the grid complies with the interconnection requirements. There are two types of grid side converter control systems, the Voltage Source Control (VSC) and the Current Source Control (CSC). VSC is the most control system applied to wind turbine, therefore it is also applied in this project.

There are two necessary blocks in VSC used in the project, the Phase Locked Loop (PLL), and the Voltage Oriented Control (VOC).

2.5.4.3 Phase Locked Loop (PLL):

The Phase Locked Loop is a subsystem that is used to get the grid voltage phase and frequency, which in turn will be used to produce a current with the same properties as the grid voltage. Figure 2.12 displays the PLL block diagram.

The PLL transfer function is:

$$H_{PLL}(S) = \frac{\theta_{inv}}{\theta} = \frac{sk_p + \frac{k_p}{T_i}}{s^2 + sk_p + \frac{k_p}{T_i}} \tag{2.29}$$

2.5.4.4 Voltage Oriented Control (VOC):

The voltage oriented control is the main part of the grid side converter control. Its main purpose is to produce a synchronized voltage signal to the PWM generator which controls the DC/AC inverter. The produced signal purpose must have two specific features, one is to have the same phase and frequency as the grid voltage, and the second feature is to have a unity power factor, which means all the power transferred from the wind turbine system to the grid is the active power, while the reactive power is controlled to have a null value. This operation can be done in various ways based on which frame is used, synchronous (dq0), stationary (αβ0), and natural reference frame.

The two common VOC schemes are based on the synchronous and stationary frames. The VOC chosen for this project is based on the dq0 components since they will be considered constant (step signal) due to the same rotation speed between the actual signals and the frame's axis, which will ease up the control scheme. The active and reactive power equations are given by (2.30) and (2.31):

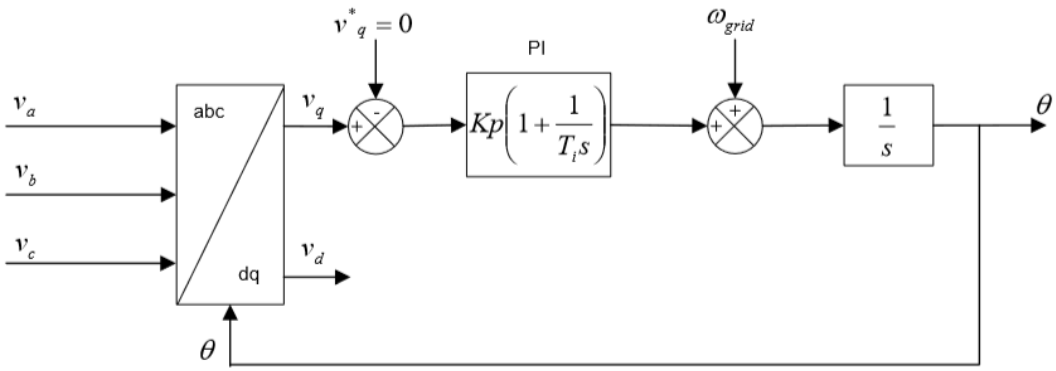

Figure 2-12: PLL block diagram [29].

$$P = \frac{3}{2} V_d i_d \tag{2.30}$$

$$Q = \frac{3}{2} V_q i_q \tag{2.31}$$

From the previous equations, it can be seen that the power components can be controlled via i_d and i_q, which are represented by the following equations:

$$\frac{di_d(t)}{dt} - w i_q(t) = \frac{1}{L}[-R i_d(t) - e_d(t) + p_d(t) v_{dc}(t)] \tag{2.32}$$

$$\frac{di_q(t)}{dt} + w i_d(t) = \frac{1}{L}[-R i_q(t) - e_q(t) + p_q(t) v_{dc}(t)] \tag{2.33}$$

The i_d* can be controlled using V_{dc} as presented in figure 2.13.

The inner loop is the current control loop, while the outer loop is the voltage control loop, the transfer function is given by (2.34):

$$H_{id}(s) = k_{pc} \frac{T_{ic}s+1}{T_{ic}s} \frac{\frac{1}{R}}{\frac{L}{R}s+1} \frac{1}{T_s s+1} \tag{2.34}$$

I_q control has only one loop which is its control loop and it will have the same parameters as i_d loop. The results will be used to produce v_d* and v_q* using PIs and sums to decouple each component from the other, which in turn will be transferred to the abc voltage components that will be fed to the PWM inputs to generate the inverter control signal. The VOC scheme is shown in figure 2.14:

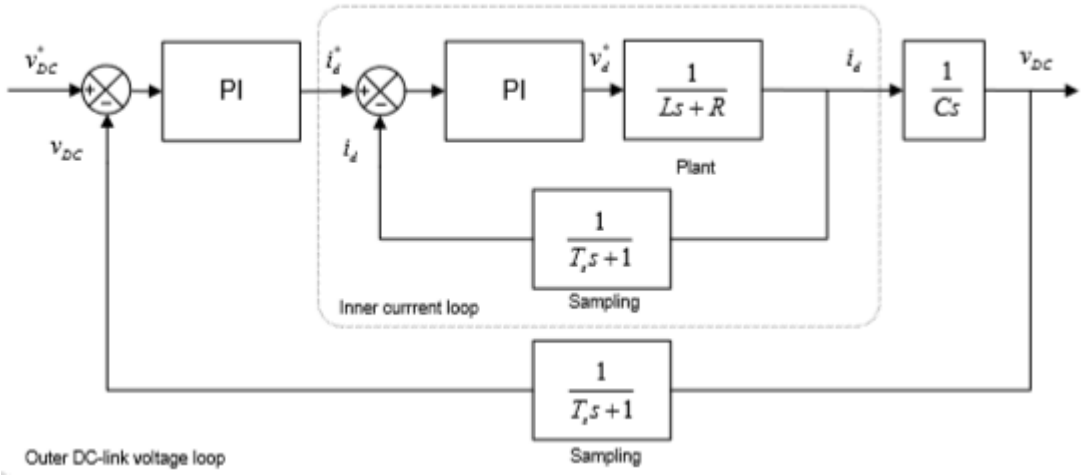

Figure 2-13: Id control loop [29].

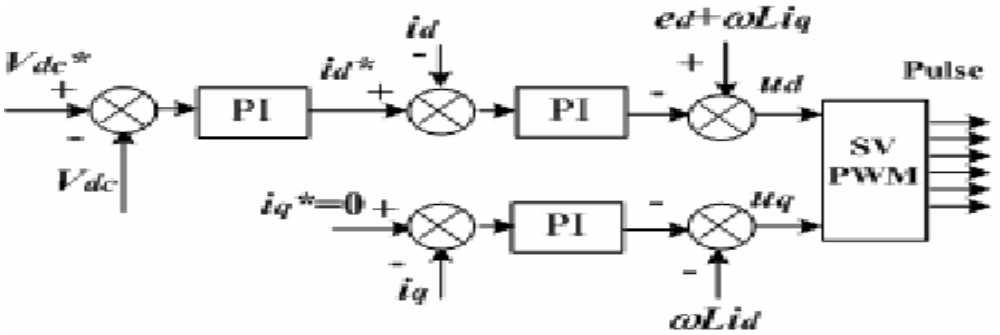

Figure 2-14: Voltage Oriented Control scheme [31].

2.5.4.5 Space Vector Modulation [29]:

The VSC requires switching status DA, DB and DC applied to the IGBT gates in order to control the power flow through the converter. SVM represents three-phase quantities as vectors in a two-dimensional α-β plane providing the duty cycles necessary for the control of the power flow through the converter. SVM is very suitable for field-oriented control, since provides accurate control of voltage amplitude, frequency and phase within every switching period. Furthermore, does not require separate modulators and calculation of zero-sequence signals as in third harmonic PWM and it has higher utilization of the DC voltage than the sinusoidal PWM method.

With SVM all three-phase waveforms are generated simultaneously which is a good advantage compared with when the phases are considered separately. The reference voltage vector is shown in the following equation:

$$V_{ref} = \frac{2}{3}(\alpha^0 V_{an} + \alpha^1 V_{bn} + \alpha^2 V_{cn}) \qquad (2.35)$$

Where α is -1/2+j3/2 and v_{an}, v_{bn} and v_{cn} are the phase reference voltages.

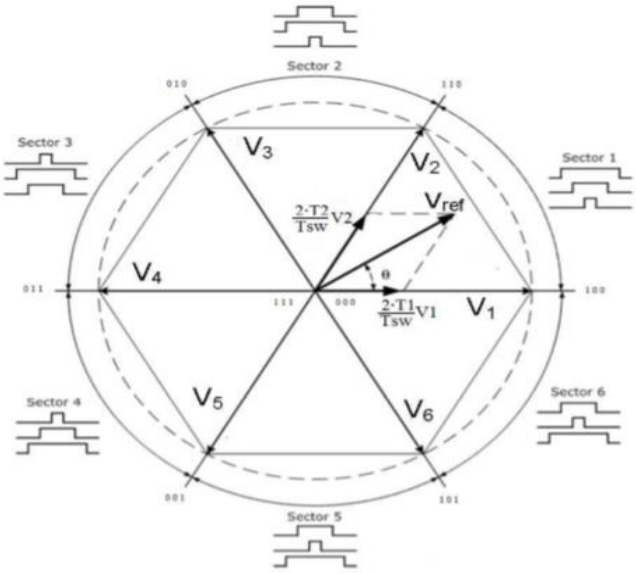

Figure 2-15: State voltage vectors and Vref represented in sector 1.

As mentioned in the previous section there are eight possible configurations for a three-leg VSC. Six of them produce a non-zero output voltage and the other two produce zero output voltage. The six non-zero voltage vectors can be represented as shown in Figure 2.15.

Each voltage vector corresponds to a switch combination of the three switching status DA, DB and DC explained previously. In Fig. 2.15 are depicted the six state voltage vectors with the needed switching status to perform them. The areas between two state vectors are sectors, hence six sectors are present. In this way the output voltage of the converter could be represented by an equivalent rotating vector V_{ref} with a counter clockwise direction, whose angle is represented by θ. Figure 2.16 shows the switching pattern for the first sector.

Where T_{sw} is the switching period. T0 is the time period left from a half switching period used by the null voltage vectors. In sector 1, the pattern used is [0 0 0], [1 0 0], [1 1 0], [1 1 1] which reduces the number of switching commutations in each transition. The time duration equation is shown as follows:

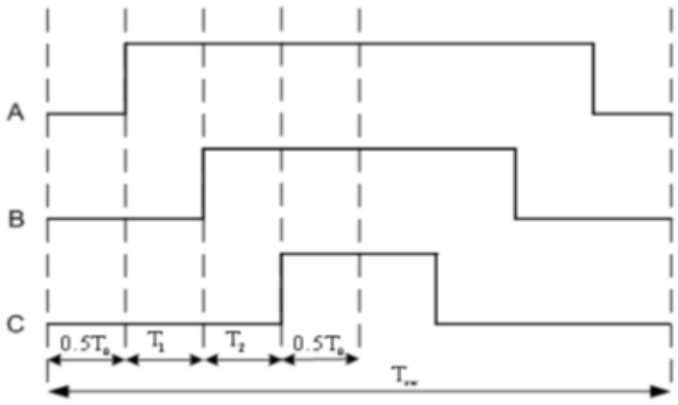

Figure 2-16: Switching pattern for the first sector.

$$\frac{T_0}{2} = \frac{T_{sw}}{2} - T_1 - T_2 \tag{2.36}$$

This reference voltage vector can be considered constant, for each switching period, if there is a high switching frequency.

Finally, in Figure 2.17 can be seen the three duty cycles a, b, c, in a complete period. The black box shows the inputs as voltages in α-β reference frame and v_{DC} as well as the duty cycles as the outputs.

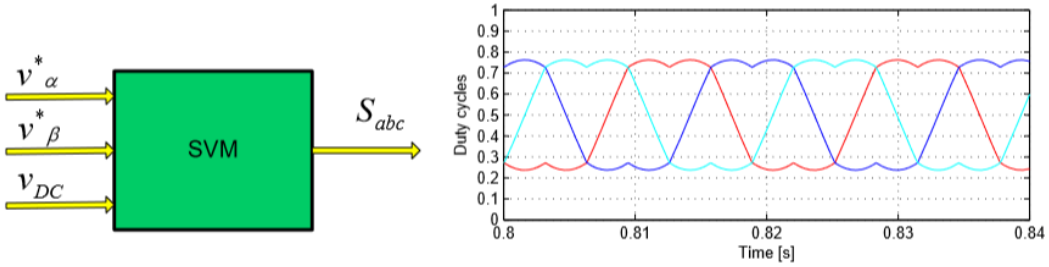

Figure 2-17: Black box and the provided duty cycles from the SVM.

In order to obtain the switching functions necessary to feed the VSC gates, PWM is necessary. PWM produces the gate signals or switching functions, by comparing the duty cycles with a carrier signal. In Figure 2.18 can be seen the black box of the PWM and the signal gates to apply the VSC.

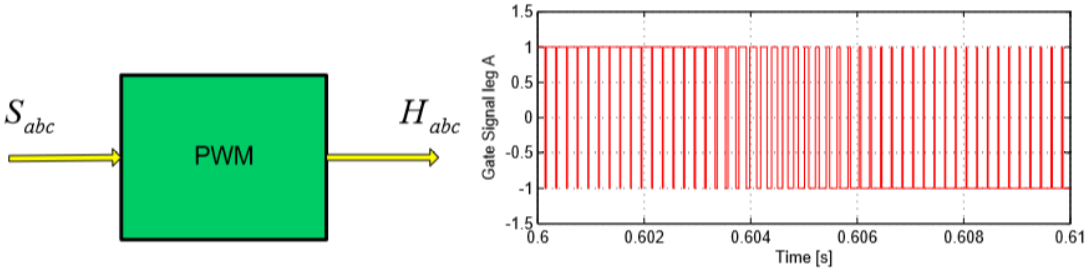

Figure 2-18: Black box and signal gates supplied by the PWM.

The relation between phase voltages and the DC-link voltage is given by:

$$\begin{bmatrix} V_{an} \\ V_{bn} \\ V_{cn} \end{bmatrix} = V_{DC} \begin{bmatrix} D_A \\ D_B \\ D_C \end{bmatrix} \quad (2.37)$$

Where v_{an}, v_{bn} and v_{cn} are the average phase voltages and D_A, D_B and D_C are the switches status at each leg respectively. The voltage between the star connection point N and the neutral point 0 is defined as in the following:

$$V_{0N} = \frac{1}{3}(V_{an} + V_{bn} + V_{cn}) = \frac{V_{DC}}{3}(D_A + D_B + D_C) \quad (2.38)$$

The phase voltages can be written as follows:

$$\begin{bmatrix} V_{an} \\ V_{bn} \\ V_{cn} \end{bmatrix} = \frac{1}{3} \cdot \begin{bmatrix} 1 & 0 & -1 \\ -1 & 1 & 0 \\ 0 & -1 & 1 \end{bmatrix} \cdot \begin{bmatrix} V_{ab} \\ V_{bc} \\ V_{ca} \end{bmatrix} \quad (2.39)$$

The current i_{dc} is expressed in function of phase currents:

$$i_{DC} = (D_A i_a + D_B i_b + D_c i_c) \quad (2.40)$$

2.6 Conclusion:

In this chapter the wind energy conversion system from mechanical power to electrical power has been presented. All parts of were discussed separately starting with the mechanical parts which included the rotor power characteristics and the drive train model, moving to the generator which is the key element in the conversion system since it converts the mechanical power to electrical power, the generator used in this project is the permanent magnet synchronous generator was discussed and its mathematical model was presented, and finally the power electronics was fully described where the voltage rectification, the boost operation, DC/AC inversion and grid connection were presented and discussed thoroughly.

CHAPTER 3 : Maximum Power Point Tracking (MPPT).

3.1 Introduction:

It is known that wind energy is continuously changing with time, and that is mostly due to the variation of its speed. This affects the power harvesting of the wind turbine since the power generated by the WECS varies with the cube of the wind speed. Therefore, in order to optimize the power extraction, the WTG needs to operate with variable speed using a control system known as maximum power point tracking system that allows the generator to operate at the optimal power point.

3.2 MPPT concept in WECS:

Maximum Power Point Tracking, frequently referred to as MPPT, is an electronic control system that allows the Wind turbine to operate in a way that guarantees the production of the maximum power that can be converted. The concept of MPPT is not mechanical in such a way where it will move the turbine to make it aligned or facing the wind direction. MPPT is a totally electronic system that varies the electrical operating point of the WTG enabling it to deliver maximum available power. Maximum Power Point Tracking (MPPT) has been used for photovoltaic (solar system) energy for a long time. But it is still a new topic in the wind energy conversion system.

Many methods to find the MPP have been developed over the past decades. These techniques differ in many aspects such as required sensors, complexity, cost, range of effectiveness, convergence speed, required hardware, and correct tracking when wind speed changes.

Among these techniques, the Perturb and Observe and the Increment conductance algorithms are the most common. These techniques have the advantage of easy implementation but they also have drawbacks such as the slow response to the change in wind speed and the long time it takes to reach the MPP. For these reasons, the algorithm that was adopted in this project is the Golden Section Search. This method is robust and also has a fast response compared to the conventional MPPT algorithms. This algorithm has guaranteed convergence under continuous variable atmospheric conditions.

3.3 Golden section search technique [14]:

Golden Section Search method is an optimization technique, discovered by the American statistician **Jack Carl Kiefer** in 1953. The concept of the technique is based on considering a function f over an arbitrary interval [a; b]. Two conditions must be met so that the technique can work, first the function f(x) has to be continuous over the interval [a; b]; and second that f(x) is unimodal over the same interval, i.e.: f(x) has only one maximum or one minimum in [a; b]. These conditions above remind us of the bisection technique and as they both have the same idea: narrow the interval that contains the maximum and comparing function values. In designing the method we seek to fulfill two goals: We want a fast reduction for the search interval and minimal number of iterations.

With these goals in mind, we are going to determine the location to evaluate the function. At first there was the choice of the bisection method would be to compute the midpoint m = (a + b) =2 and to evaluate at x1 and x2, defined by x1 = m – delta/2 and x2 = m + delta/2, for some small value of delta such that $f(x1) \neq f(x2)$. If f(x1) < f(x2), then we are left with [a; x1], otherwise [x2; b] is our new search interval. While this halves the search interval in each step, we must take two new function evaluations in each step and this is not optimal.

The GSS technique was introduced as a counter part of bisection for finding roots of equations, by optimizing the performance to one new function evaluation in each step. Furthermore, the golden section search method only depends on one constant reduction factor, say R as shown in fig.3.1, for the size of the interval. For x1 and x2 somewhere in [a; b], there are two cases:

1. If f(x1) < f(x2), then interval [a; b] becomes [x1; b], with interval size reduction:

$$2 - a = R(b - a) \quad \ldots\ldots\ldots \tag{3.1}$$

$$x_2 = Rb - Ra + a \quad \ldots\ldots\ldots \tag{3.2}$$

$$x_2 = a(1 - R) - Rb\ldots\ldots\ldots \tag{3.3}$$

2. If f(x1) < f(x2), then [a; b] will become [x1; b], with interval size reduction:

$$b - x1 = R(b - a) \quad \ldots\ldots\ldots \tag{3.4}$$

$$x_1 = Rb + Ra - b \quad \ldots\ldots\ldots \tag{3.5}$$

$$x_1 = b(1 - R) + Ra\ldots\ldots\ldots \tag{3.6}$$

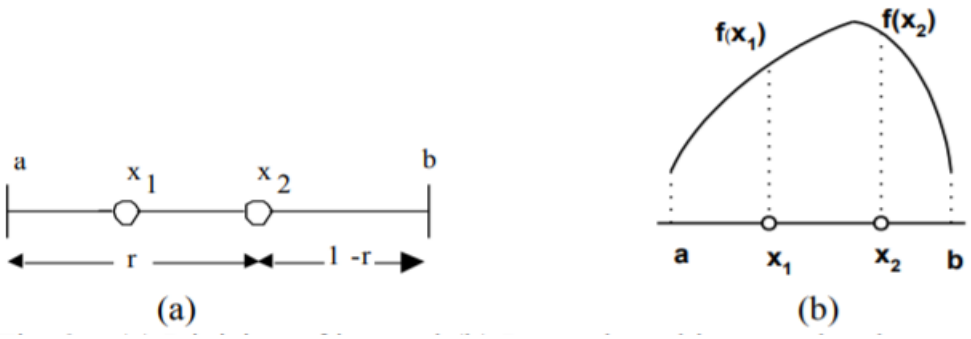

Figure 3-1: Golden section search method [32].

Thus, by giving a value to R, we'll be able to locate both of x_1 and x_2. In order to find the value of R, we take on the case f(x1) < f(x2). For easy of calculation, take choice of the interval is [a; b] = [0; 1].

Now assuming that $f(x_1) > f(x_2)$, we set b ←x_2 otherwise we put a ←x_1, which yields a new interval [a; b] reduced by a factor R, as illustrated. To carry out the next iteration we calculate the new points $f(x_1)$ and $f(x_2)$ in the new interval, and repeat the process.

The procedure works only if the same constant R locates X_1 and X_2in both intervals. Saying that $f(x_1) > f(x_2)$, so we place a new function evaluation in the interval [a; x_2] which is equal the interval [0; R], and we write x1 in two ways (using the formula for x_2 derived above with a =0; b =x_2= R) and with:

$$x_1 = 1 - R \tag{3.7}$$

$$1 - R = (1 - R) \times 0 + R \times R \tag{3.8}$$

Which yield to:

$$R^2 + R - 1 = 0 \tag{3.9}$$

The positive root leads to the golden ratio:

$$\mathrm{R} = (-1 + \sqrt{5})/2 = 0.618033989 \tag{3.10}$$

Where R is the ratio of the sides of a "golden rectangle," considered by ancient Greeks to have the perfect proportions.

The process is continuously repeated until the difference $|X_2\text{-}X_1|$ becomes less than a certain chosen precision, the resultant maximum's abscissa is given at point:

$$X_0 = \frac{1}{2}(X_1 + X_2) \tag{3.11}$$

The number of iterations required to reduce the interval from $|b-a|$ to an error tolerance say ε is given by:

$$|\text{b-a}|\,R^n=\varepsilon$$

(3.12)

Giving:

$$n=\frac{\text{Ln}(\varepsilon/|\text{b}-\text{a}|)}{\text{LnR}}=-2.078087\ \text{Ln}\ \frac{\varepsilon}{|\text{b}-\text{a}|} \qquad (3.13)$$

The whole technique is described on the flowchart given in fig.3.2.

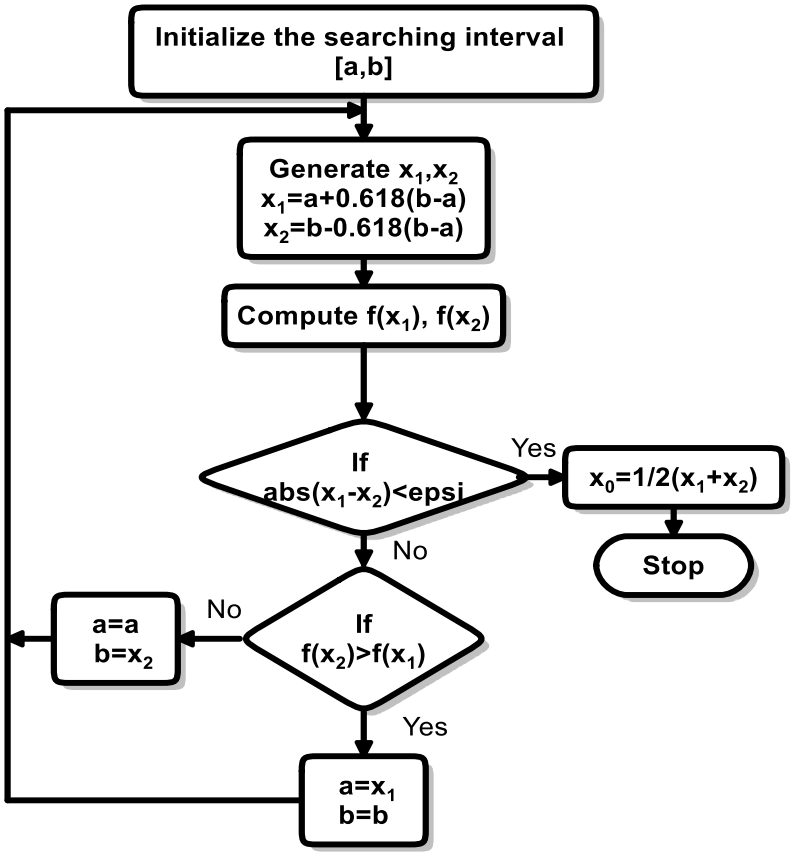

Figure 3-2: Flowchart of golden section search algorithm.

3.4 Adaptation of golden section search on MPPT:

Fig.3.3. shows the configuration of the proposed MPPT.

Since, the wind speed varies continuously and the load changes continuously. And in order to match the load with the wind energy conversion system, a power electronic interface is required between the wind energy conversion system and the load.

This power-conditioning unit consists of three main blocks, Rectifier (AC-DC), DC-DC boost converter and Inverter (DC-AC). The power electronic interface

is used, in order to ensure an optimal operation of WECS; which is achieved by controlling the duty cycle of the boost converter in the system.

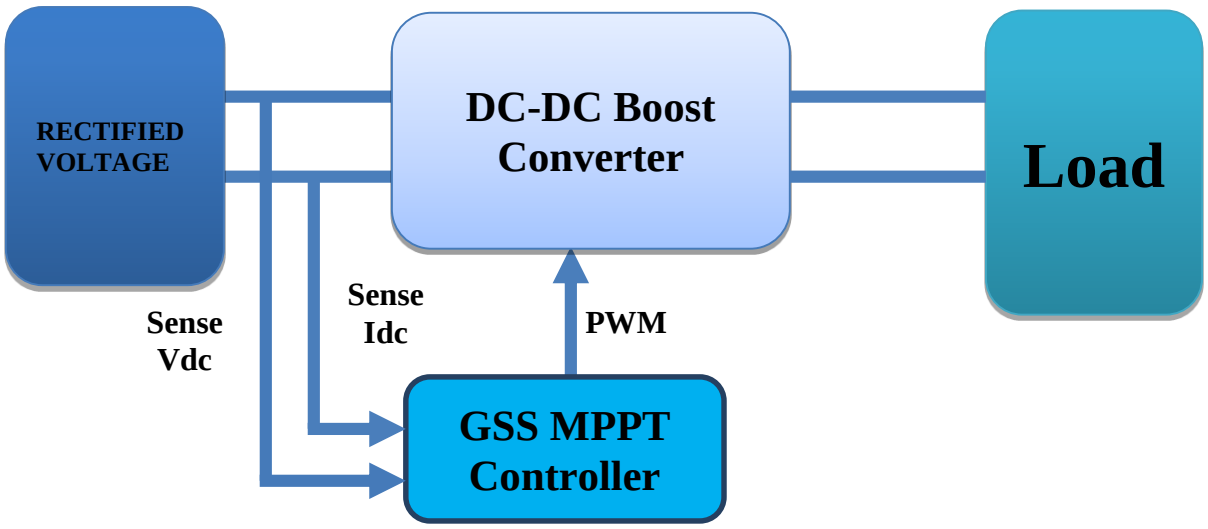

Figure 3-3: Configuration of the MPPT control.

load. In order to extract the maximum power from the wind, the duty cycle of the boost converter is controlled by the MPPT algorithm. And, by maximum power transfer theorem, a source will deliver its maximum power when the source impedance matches the load impedance. The duty cycle of the converter is maintained in such a way that the effective impedance seen by the wind energy conversion system source will be equal to the internal source impedance, hence maximum power is delivered. Figure below represents the typical curve of wind power variation according to the operating speed of the generator which is proportional to the voltage rectified. Fig3.4 shows that there is an optimum rotating speed to get the maximum wind power under certain wind speed.

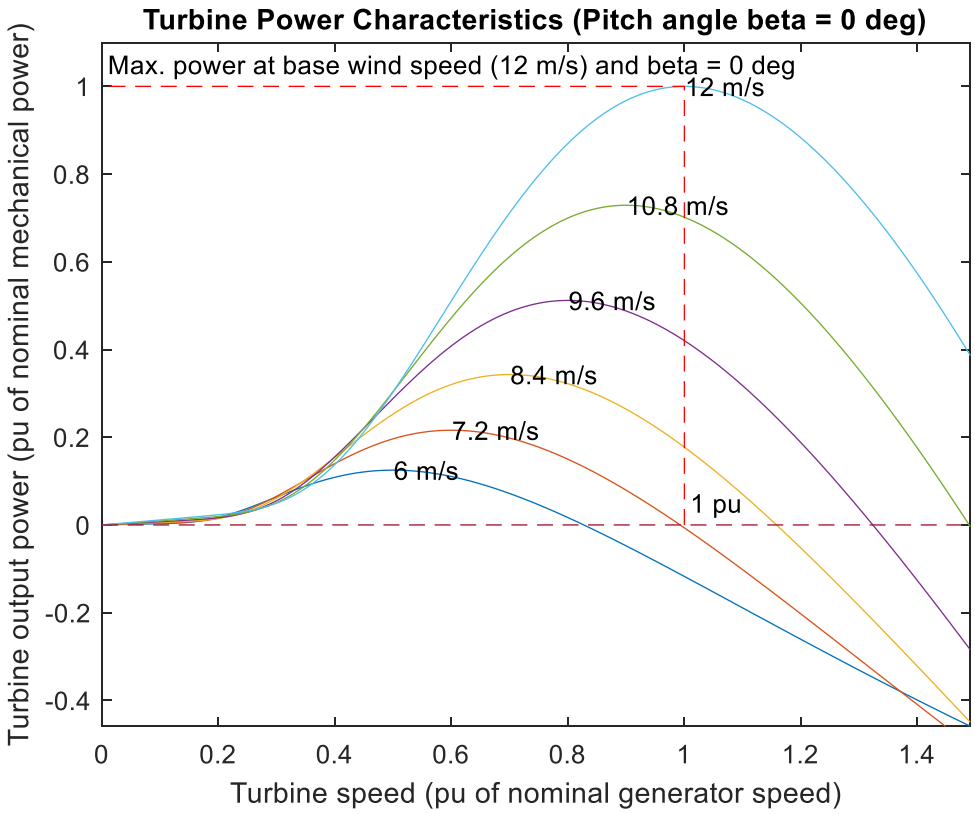

Figure 3-4: Power versus generator speed of WT.

Now by making the GSS as the MPPT algorithm. By taking the power generated by the WTG as the function f(x) and the DC voltage as the changing variable, and since the power curve of the WT satisfies the GSS conditions, the algorithm will be set start by first to setting an interval.

[a; b] that varies from a medium voltage value to the maximum voltage that can be attained by the generator, after that two voltage values V_1, $V_2$are generated from the starting interval such that:

$$V_2 = a + 0.618(b - a) \tag{3.13}$$

$$V_1 = b - 0.618(b - a) \tag{3.14}$$

The power values at these voltages $P(V_1), P(V_2)$ are measured using the output V_{dc} and I_{dc} from the rectifier. They are compared and accordingly the search interval is shrunk from right or left. Another voltage values for $V_1$and $V_2$from the resultant interval are generated; its power is then measured and compared as done in the previous iteration. The process is continued until the MPP is reached, that is when $|V_2\text{-}V_1|$ is less than a chosen precision delta. Once the MPP is reached, the optimal

voltage is fixed and equals $V_{mp} = \frac{1}{2}(V_1 + V_2)$ and the system is forced to operate at that point. The flowchart of the proposed method is shown in fig 3.5.

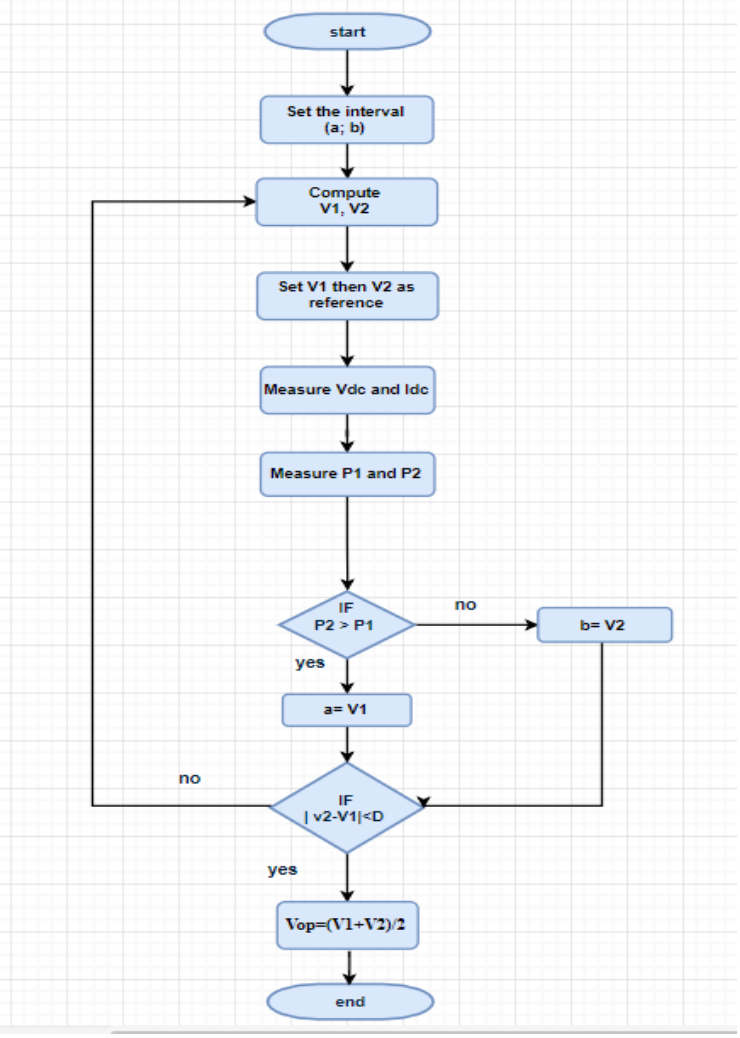

Figure 3-5: Flowchart of the MPPT algorithm based on GSS.

3.5 Conclusion:

In this chapter we introduced the concept of the maximum power point tracking, what it means MPP, how to find it, and the factors responsible for changing it. We also explained the MPPT algorithm we used in this project which is the Golden Section Search method by demonstrating the way it works and how to implement it in our WECS.

The next chapter will be dedicated to the simulation results and the discussion of our system.

CHAPTER 4 : Simulation and Results.

4.1 Introduction:

The previous chapters, described the modern wind turbines, the electrical generators used in WECS, also it been talked about the main components responsible for the power conversion in the variable speed WT, such as power electronics and control systems used for optimizing the power extracted (MPPT algorithm), and for grid connection (voltage oriented control). The power electronic interface is used, in order to ensure an optimal operation of WECS.

This chapter will be dedicated to discuss the simulation results of this system obtained from MATLAB/SIMULINK software.

4.2 System configuration:

In this section a MATLAB-SIMULINK model of the WECS and the control systems are first presented.

The wind power conversion system consists of a wind turbine block connected to a permanent magnet synchronous generator through a two mass drive train as shown in fig.4.1. Additionally The wind turbine and the PMSG and are given in tables 4.1, 4.2 respectively.

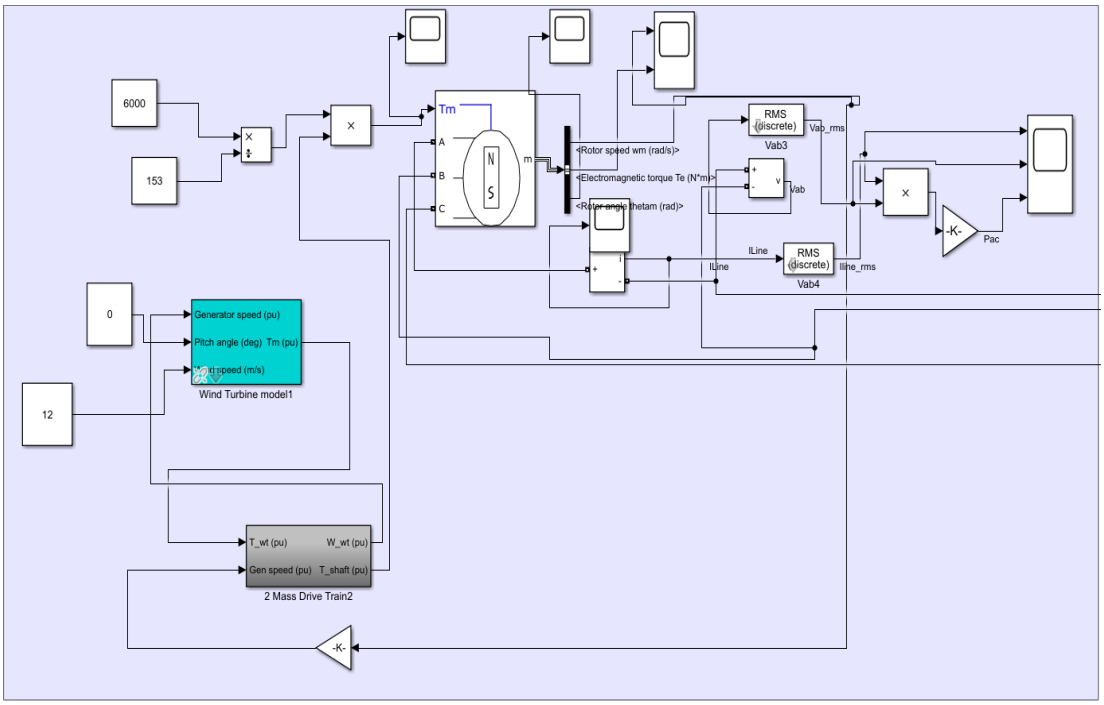

Figure 4.1: Wind power generation model.

Table 4-1: The parameter of wind generator.

Characteristics	Values
Nominal mechanical Output Power (P)	8.5 kW
Base power of electrical generator	6 kW
Base wind speed	12m/s
Max pu power at base wind speed	0.82
Base rotation pu speed	1
Pitch angle	0

Table 4-2: The parameter of the PMSG.

Characteristics	Values
Stator phase resistance R_S (ohm)	0.425
Inductances L_d ,L_q (H)	0.0082
Flux linkage established by magnet (V.S)	0.433
Rated speed (rad/s)	153
Base power (W)	6 kW
Number of poles pairs(n_p)	5
Inertia Kg.m^2	0.01197
Friction factor N.m.s	0.001189
Base torque (N.m)	40

The power-conditioning unit consists of three main blocks, uncontrolled Rectifier (AC-DC), DC-DC boost converter and a two level Inverter (DC-AC), in addition to the control system, as illustrated in fig.4.2.

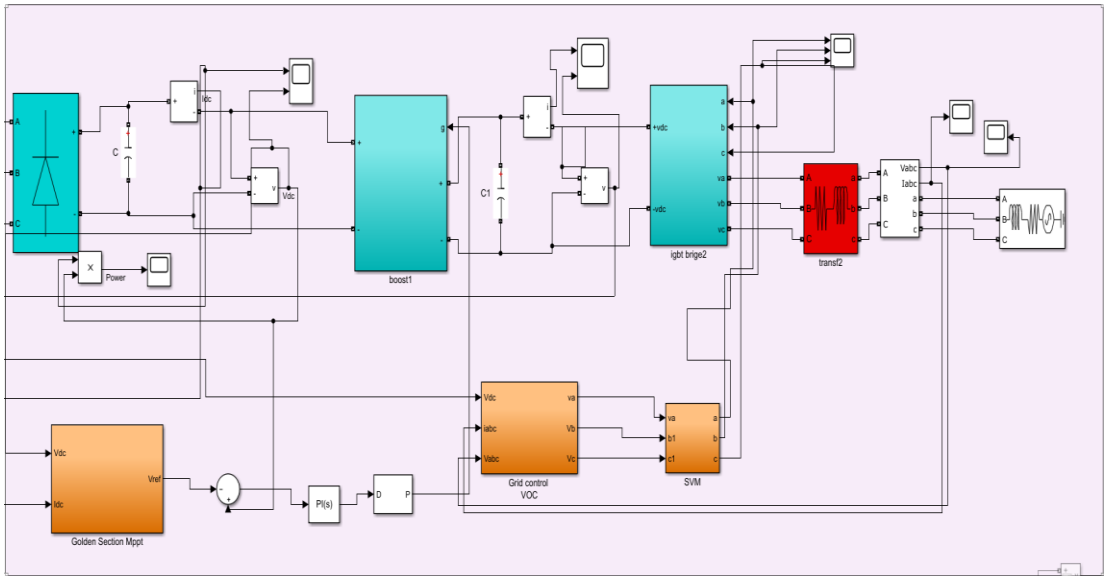

Figure 4.2: Power interface configuration.

The boost converter parameters are shown in the table 4-3.

Table 4-3: The parameter of the boost converter.

Characteristics	Values
Inductance (H)	3.5
Input capacitor (mF)	3
Output capacitor (mF)	0.336
Diode	Ideal

For the utility grid the parameters that have been chooser are mentioned in the table 4-4.

Table 4-4: The parameter of the utility grid.

Characteristics	Values
Phase-to-phase voltage (Vrms) (V)	380
Frequency (Hz)	50
RL Filter (H, Ohm)	0.1/ 15

4.3 Simulation and results:

The simulation process was carried on three parts:

4.3.1 Machine side:

4.3.1.1 System simulation without MPPT algorithm:

For the wind speed two values were chosen, first 12 m/s which is the optimal wind speed, and second 10 m/s.

Simulation of the WECS without MPPT algorithm, was modeled but connecting the wind power generator to a DC load through a three phase uncontrolled rectifier

The load chosen for this part is: R= 50 ohm, knowing that the generator delivers connected to this load the following values:

V_{dc}= 550 V , I_{dc}= 11 A and a dc output power P= 6100 W

An interval of 10 s was taken as time of simulation in which the wind speed was 12 m/s in the interval [0, 5] and from [5, 10] the wind changed to 10m/s.

The resulting curves for each of the output power, rotor speed, and the rectified voltage and current signals are shown in the fig (4.3 – 4.5).

Wind speed 12 m/s:

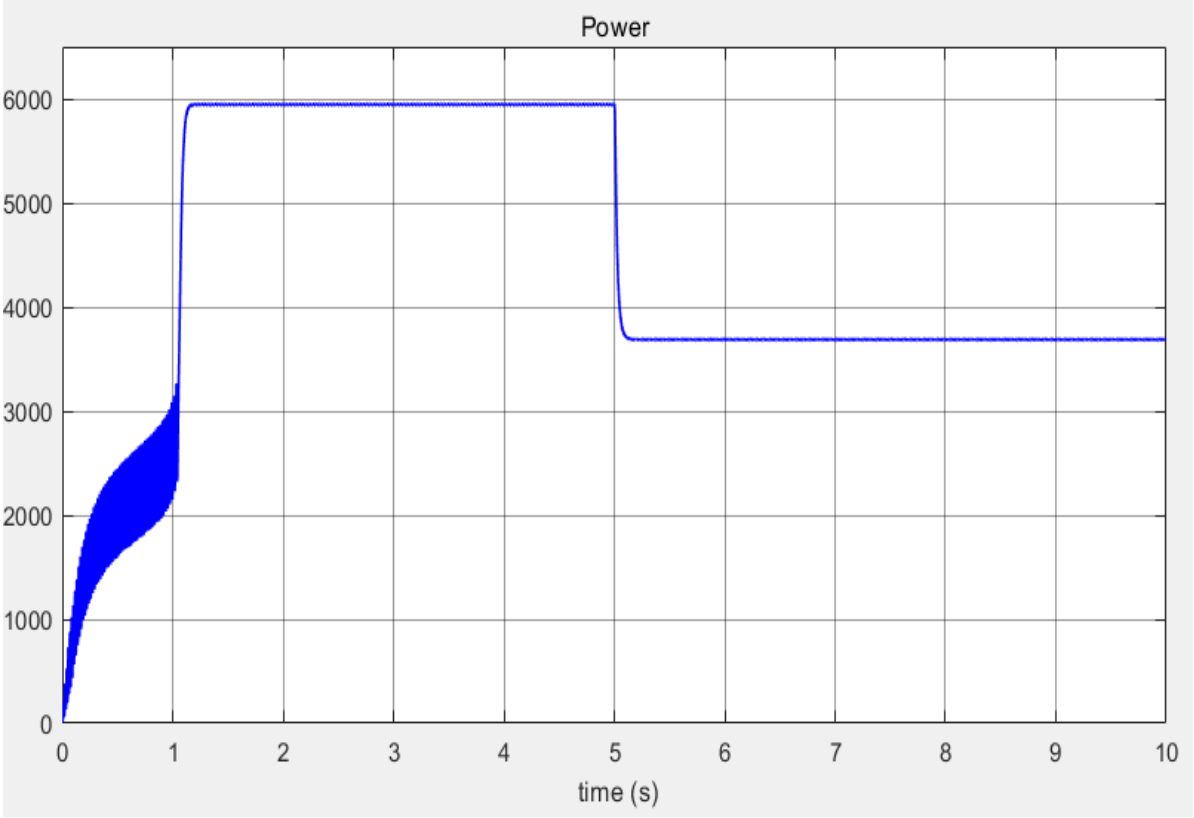

Figure 4.3: Output dc power.

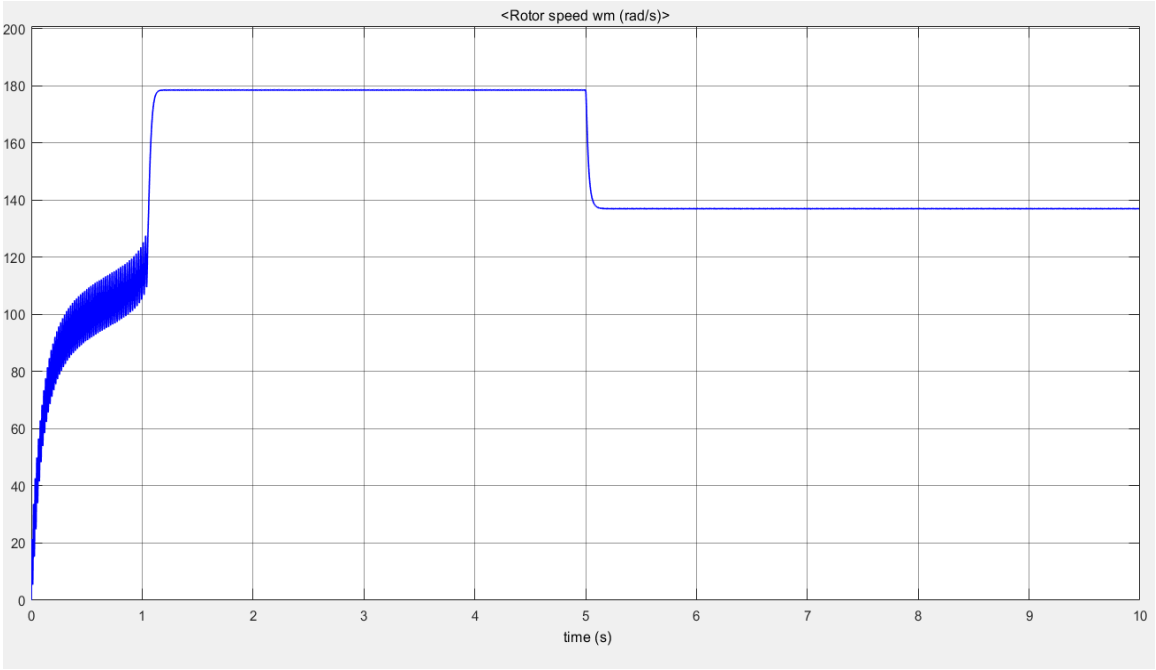

Figure 4.4: Generator rotor speed.

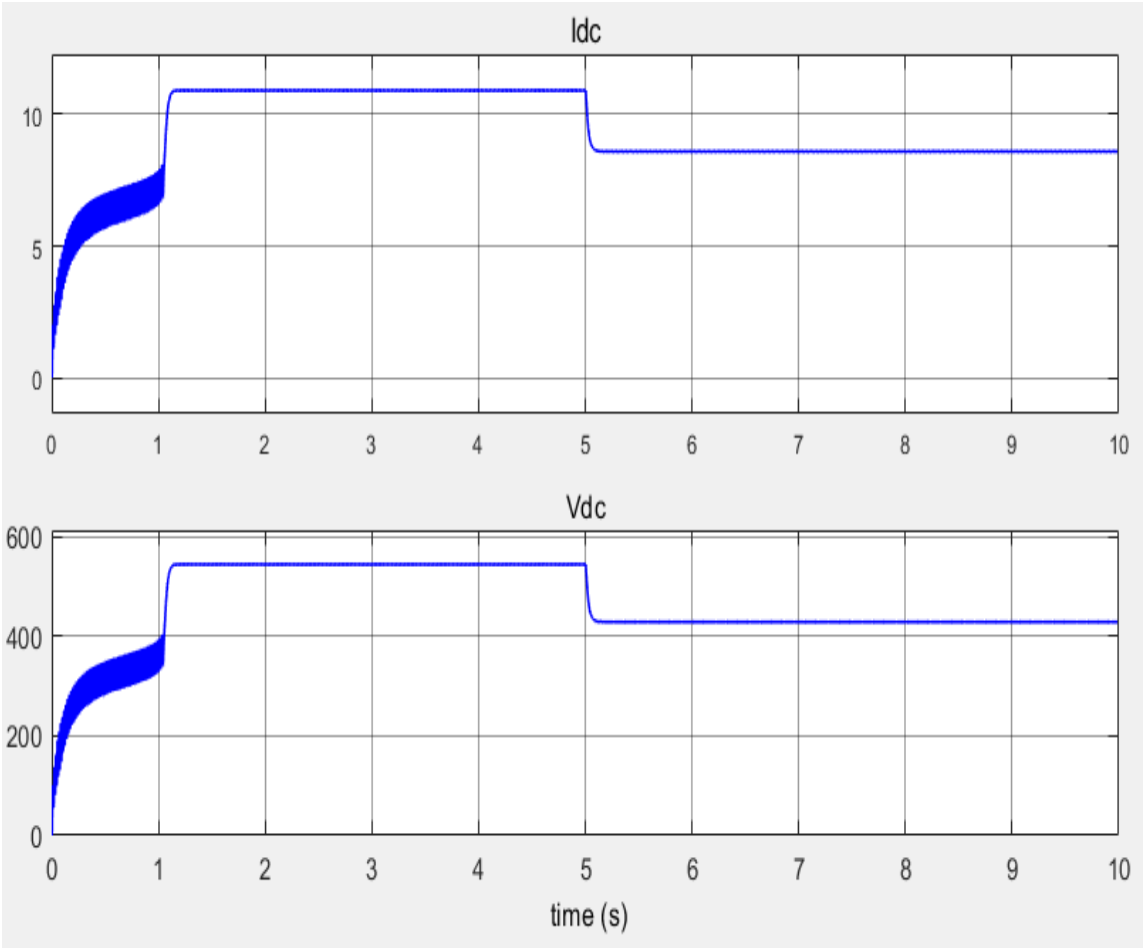

Figure 4.5: Voltage and current curve.

4.3.1.2 System simulation with MPPT algorithm:

At the same conditions as the first simulation (same wind speeds and pitch angel), this simulation of the system using the MPPT controller took a place the simulation time chosen is 10 s.

The GSS MPPT algorithm parameters selected were as following:

- The interval of the search: a= 250 V and b= 580 V.
- The accuracy is delta= 10V.

The resulting curves are shown in figures (4.6-4.8).

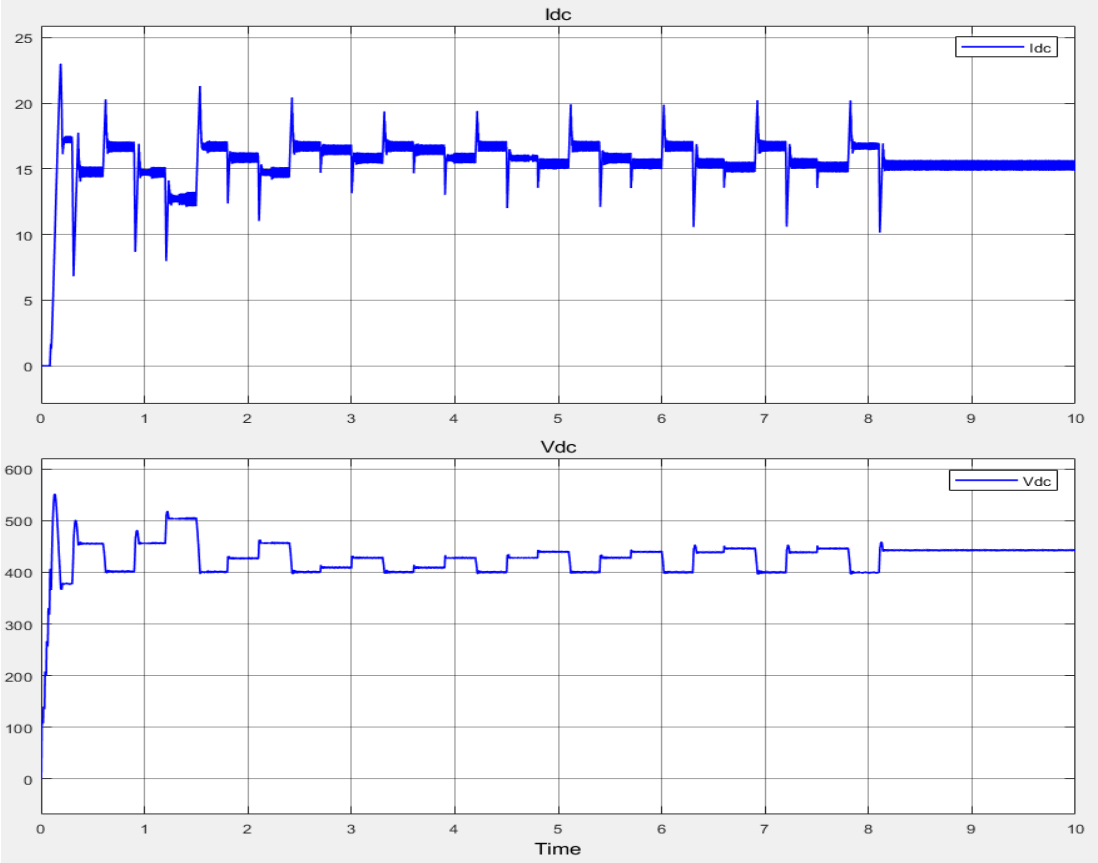

Figure 4.6: MPPT Voltage and current curve at 12 m/s.

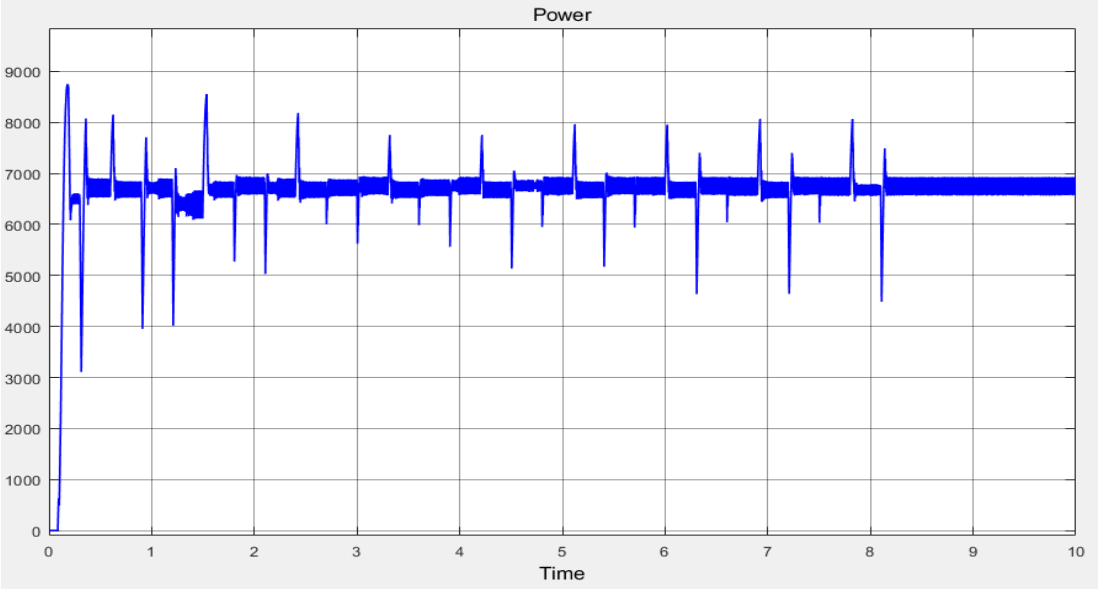

Figure 4.7: MPPT Output dc power at 12m/s.

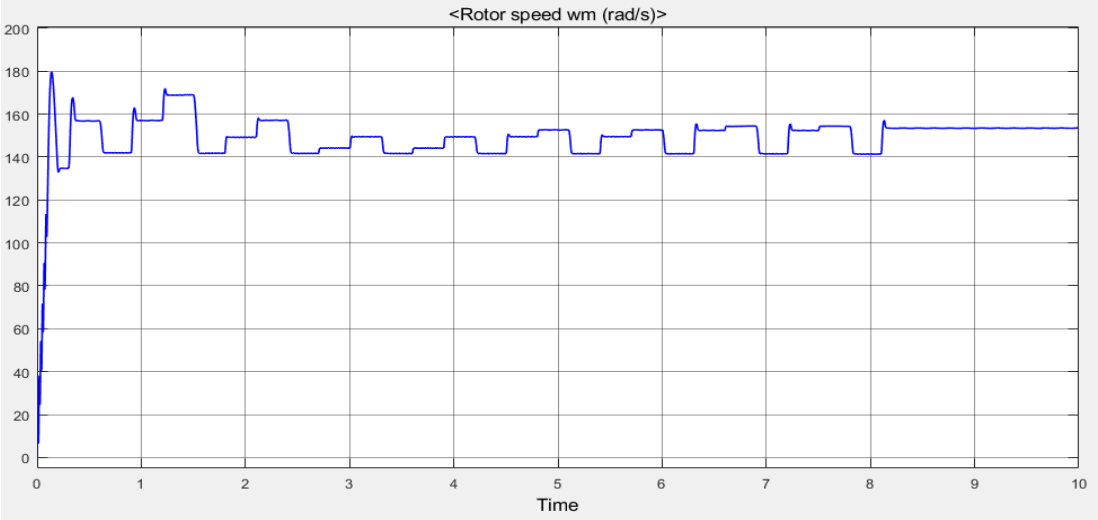

Figure 4.8: MPPT Generator rotor speed at 12 m/s.

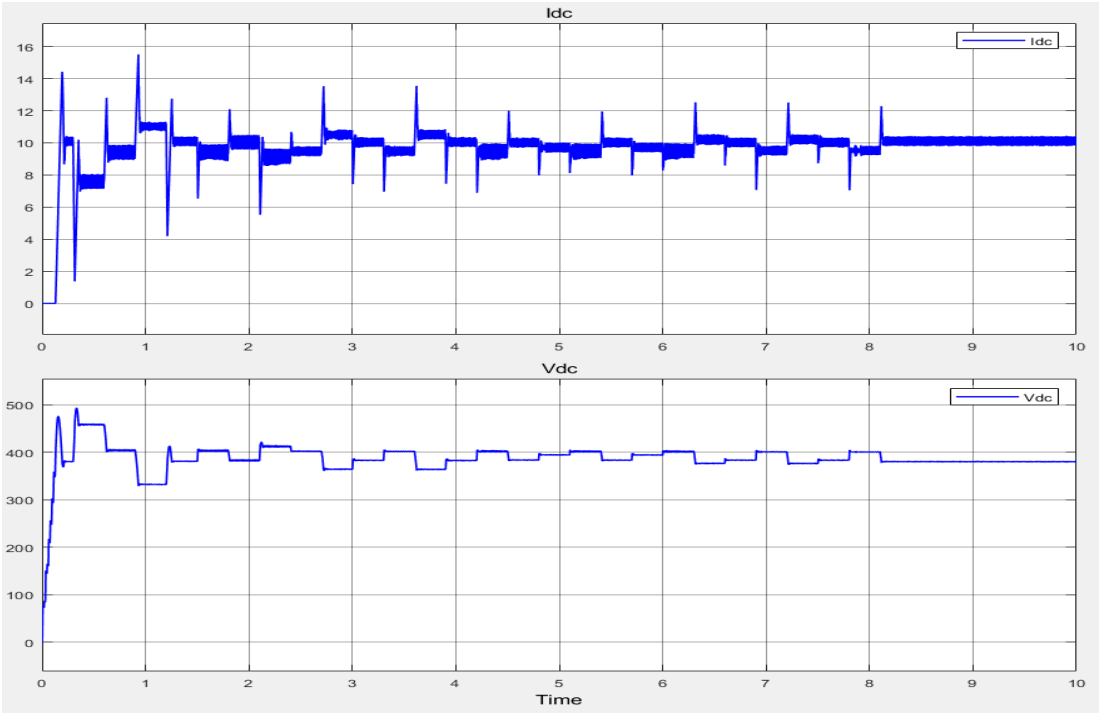

Figure 4.9: MPPT DC voltage at 10 m/s.

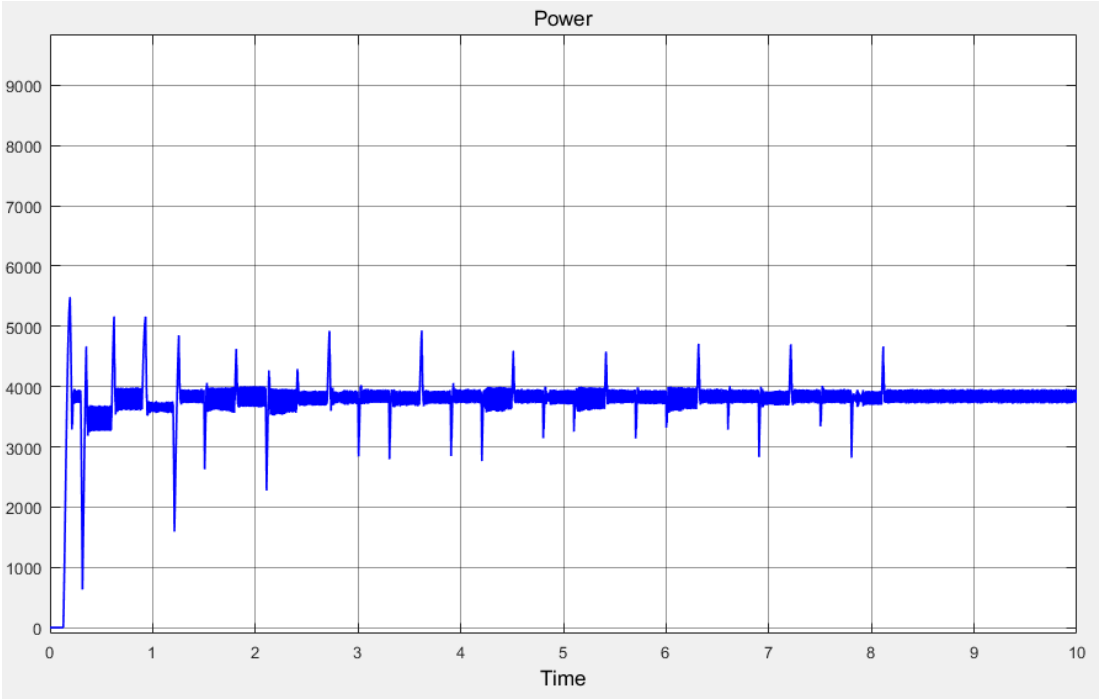

Figure 4.10: MPPT Power curve at 10 m/s.

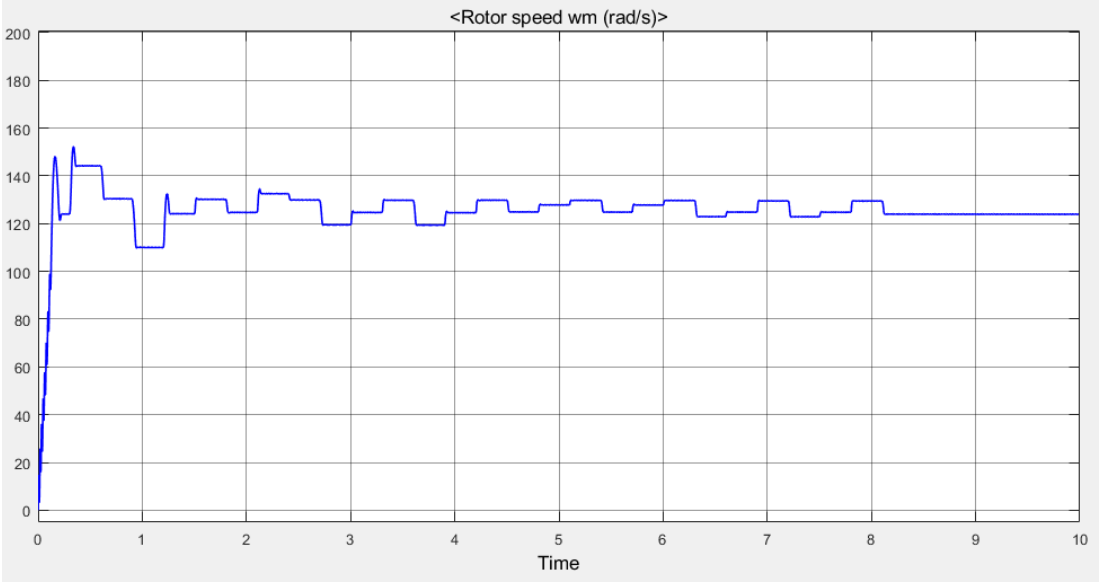

Figure 4.11: MPPT rotor speed at 10m/s.

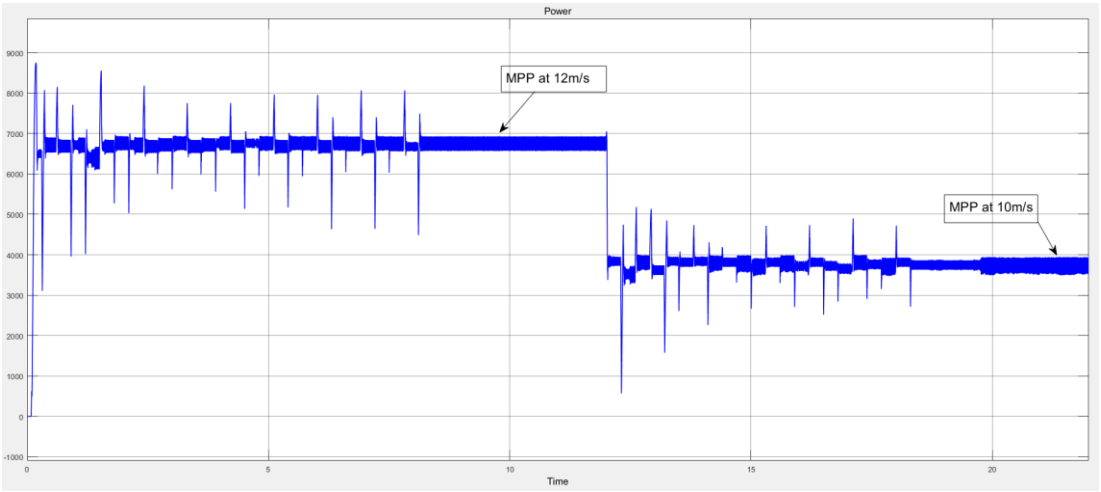

Figure 4.12:MPPT Power curve.

4.3.2 Grid side:

In this part, the simulation results were obtained with open loop control. The choice of the grid phase to phase rms voltage is 380 V, with frequency 50Hz. The resulting curves are shown below:

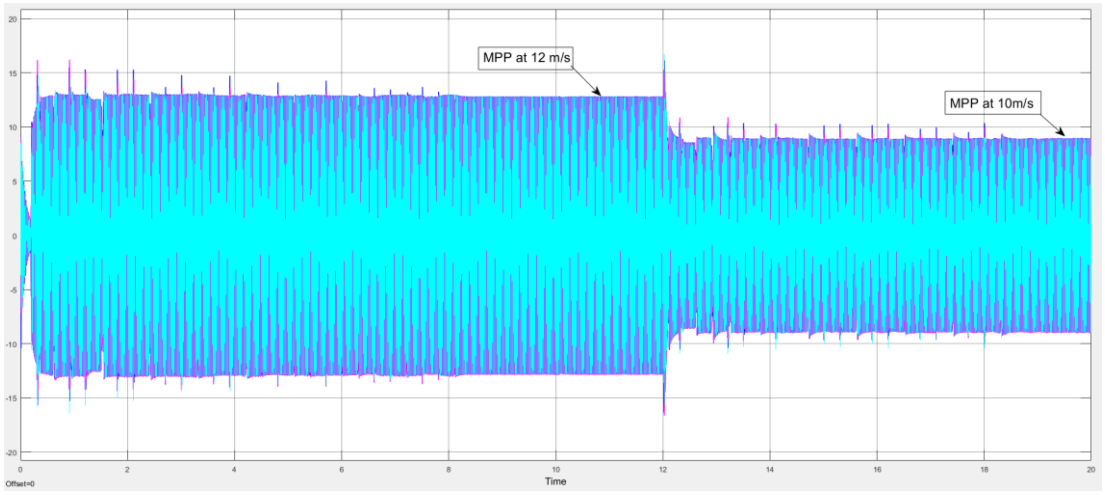

Figure 4.13: Grid side current.

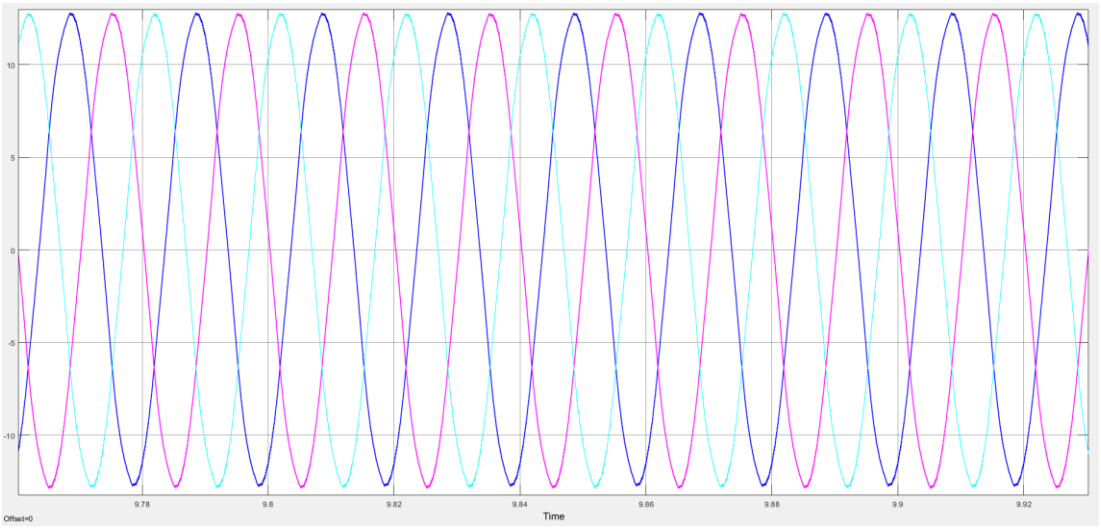

Figure 4.14:Grid side three phase current at 12 m/s.

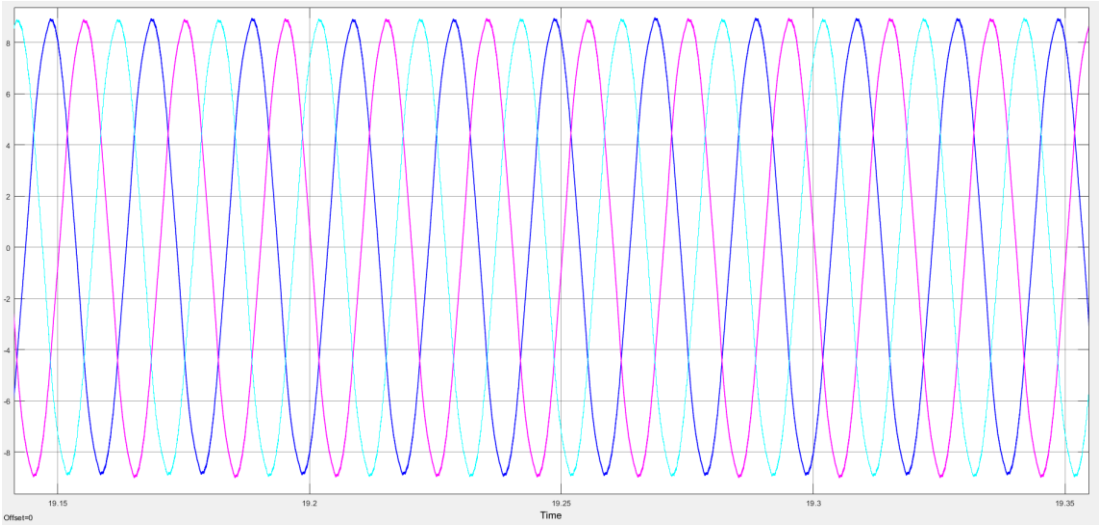

Figure 4.15: Grid side three phase current at 10 m/s.

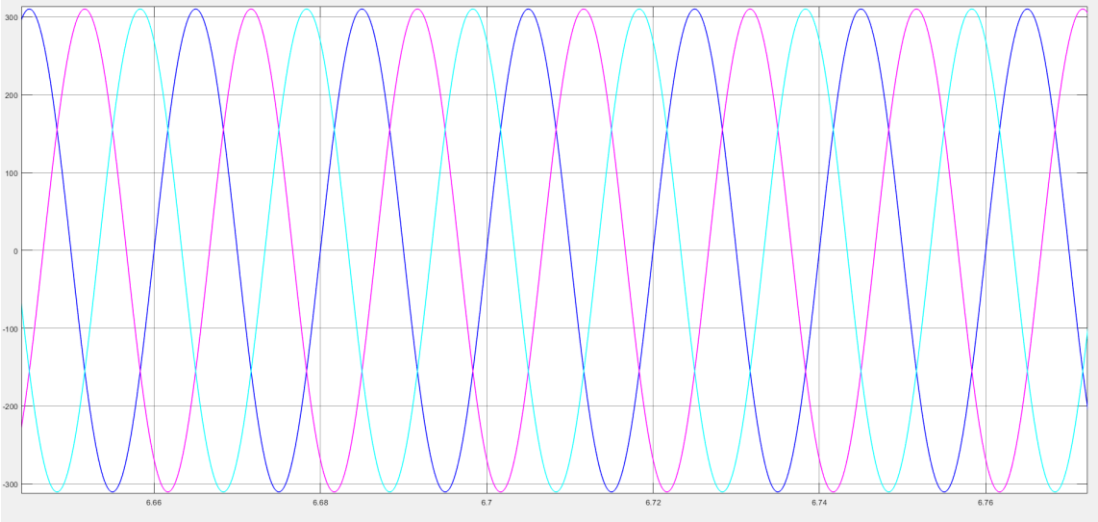

Figure 4.16: Grid voltage.

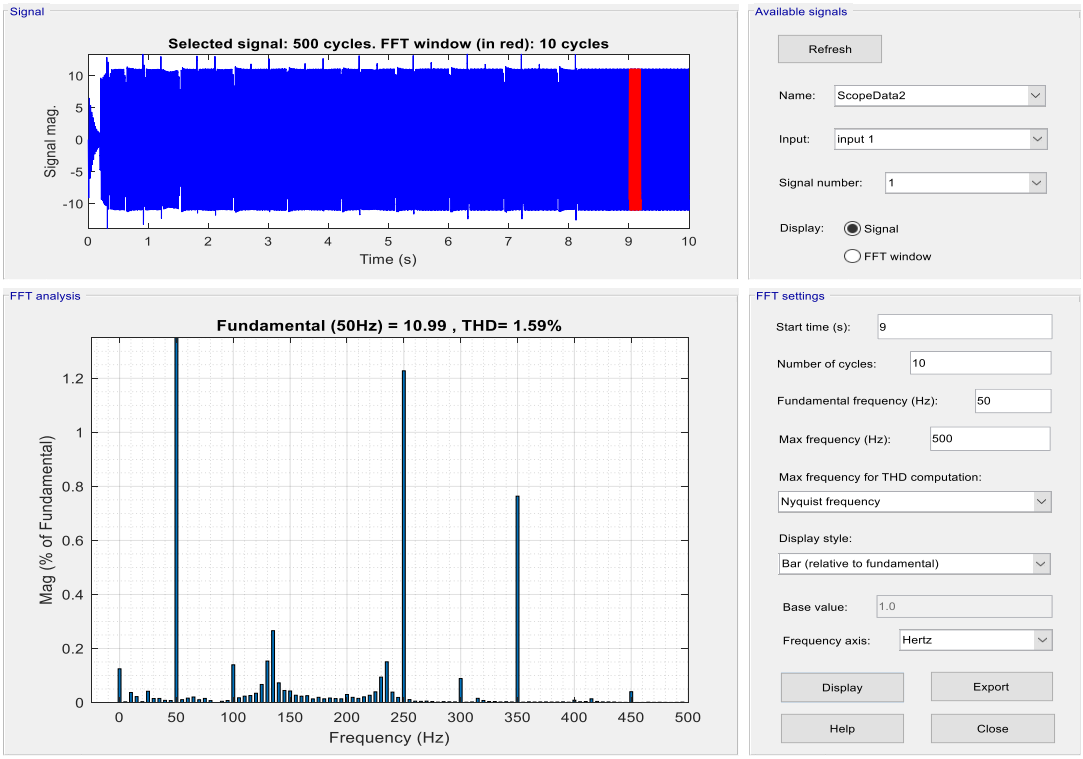

Figure 4.17: THD of the grid current.

4.3.3 Perturb and Observe MPPT simulation results:

The GSS MPPT controller was replaced by the P&O MPPT algorithm in order to compare the two methods. The simulation results are shown in the figures (4.18-4.21):

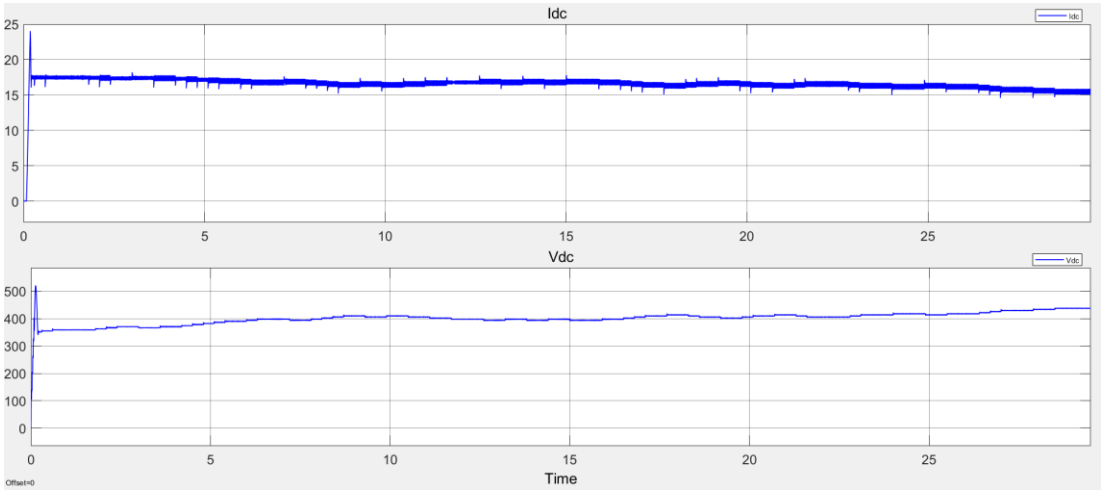

Figure 4.18: Voltage and current curve with P&O MPPT.

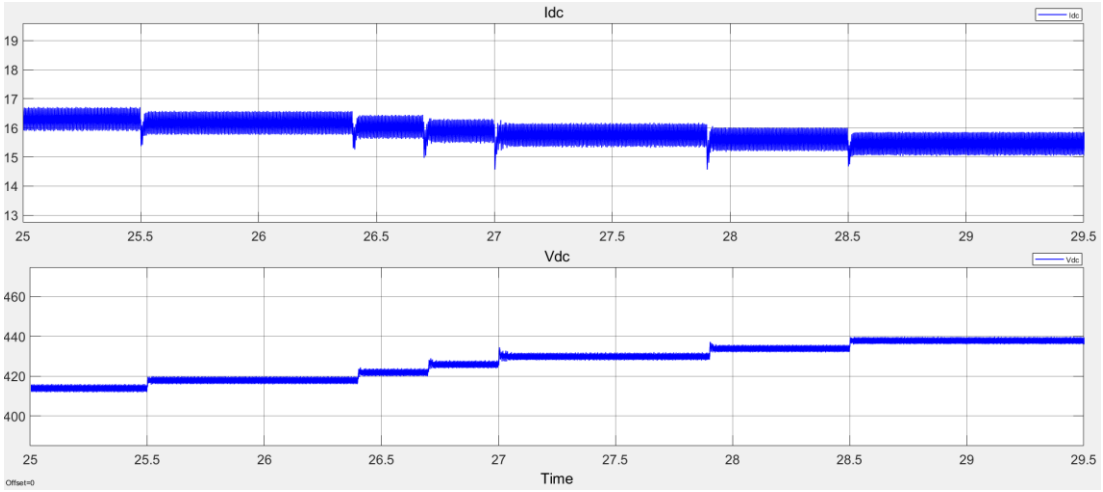

Figure 4.19: Zoom on the MPP of voltage and current curve with P&O MPPT.

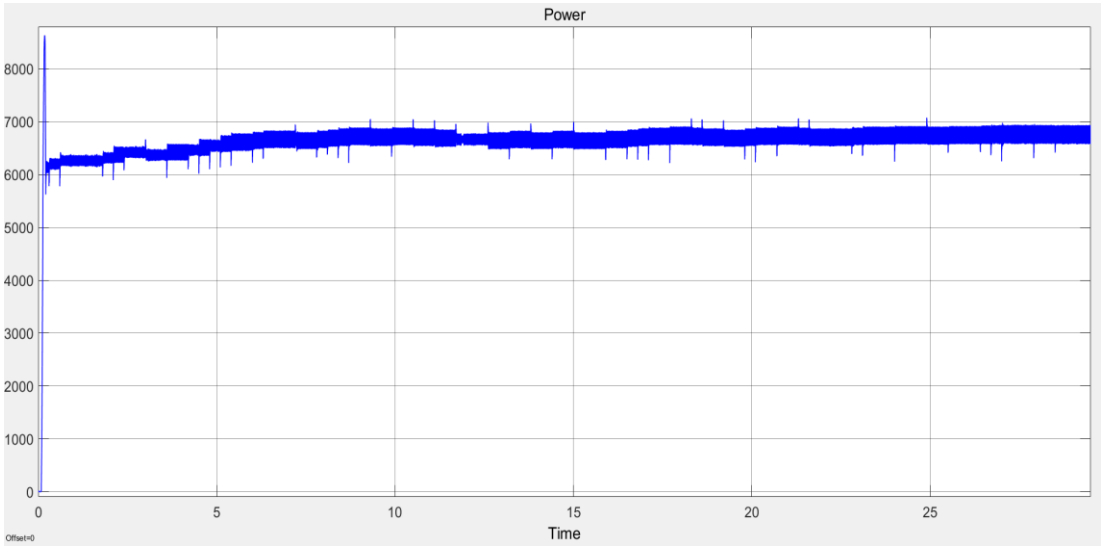

Figure 4.20: The power curve with P&O MPPT.

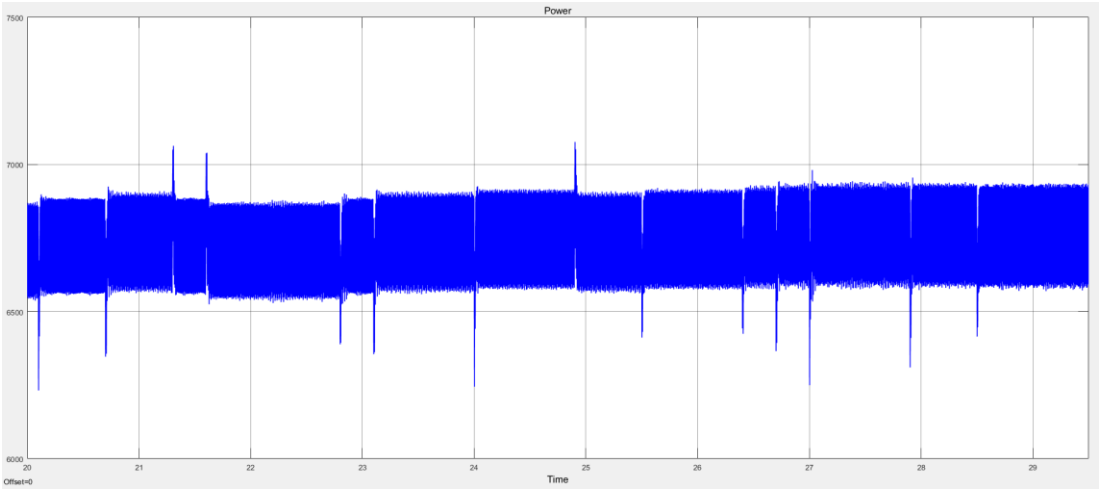

Figure 4.21: Zoom on the MPP of power curve with P&O MPPT.

4.4 Discussion and comments:

Based on simulation results the discussion will focus on two main parts:

4.4.1 Machine side:

4.4.1.1 Without MPPT control:

As it is seen in the figures (4.9-4.11), the WECS operated at a variable wind speed equals to 12 m/s from 0 s to 5 s at 10m/s from 5 s till 10 s without the MPPT control, it is noticed that the PMSG operates at a rotor speed 178 rad/s which is 1.16 p.u. the base speed, and it generates a constant three phase current and voltage that give after rectification (AC/DC) a DC current and voltage signals 11 A and 550 V respectively, with an output power equals to 6000 W. It is clear that the WTG is supplying lower power than its base power 7000 W. Based on power curve versus rotor speed graph, there is a nonlinear relationship between both variables. As seen previously there is an optimal rotor speed in which enables the generator to deliver optimal power. In this system, the optimal power expected to be extracted at 12m/s wind speed is 0.82 p.u the wind turbine's mechanical power (8.5kW), and since the generator rotate at 1.16 p.u. it caused the WECS to extract less power than the rated power. The same case is viewed when the wind speed decreased to 10 m/s, the rotor speed is 137 rad/s which equals 0.9 p.u. the optimal speed at this wind speed value, 122.4 rad/s; consequently, the WECS is operating at the point where V_{dc}=430V, and

I_{dc}= 8A delivering a power of 3600 W, which is less power comparing to the optimal power at 10 m/s wind speed.

4.4.1.2 With MPPT control:

Figures (4.6-4.12) display the results. For both wind speed equals 12m/s, and 10 m/s.

The rotor speed settles on 149 rad/s, the DC signals settle on 15.5 A and 443 V. The power obtained is 6900 W. As noticed, the MPPT controller succeeded to locate the MPP after seven iterations in 8.1 s. The response time taken by the system in order to find the MPP is good taking into consideration that each transient phase in order for the generator to operate at a reference voltage giving by the MPPT controller takes 0.3 s.

Looking back at the results of the system without the MPPT controller, the power extraction was optimized by 900 W. This improvement is due to the fact that the first system (without control) is only connected to a DC load, which means that the system was set to work on a single point in the power curve. On the other hand the MPPT controller allowed the system to work in different points by using the load matching principle, converging to the MPP. Now for 10 m/s wind speed, the same results where noticed in which the power extraction improved from 3600W to 3900W.

Knowing that the maximum power that the generator can deliver at both optimal wind speed 12m/s and 10m/s is 7 kWand 4080 kW respectively, comparing to the results obtained by the controller, the values are very close. With an efficiency 98% at 12 m/s and 96% at 10 m/s.

4.4.2 Grid side:

The results obtained above are based on open loop control with only SVM attached to the DC/AC two level inverter through a PWM, the frequency of the SVM equals 50 Hz. In other words, the VOC was not taken under consideration; so, the grid synchronization and active and reactive power control were not designed for this system. As noticed the current curves change according to the power supplied to the inverter. At 12m/s, the i_{abc} amplitudes reach 13 A, and at 10 m/s the amplitudes reach 9 A. The THD reaches to 1.59% which is satisfactory knowing that the THD limit must be less than 5% in order to connect the system properly to the grid utility.

4.4.3 P&O MPPT controller:

The simulation results shows that his MPPT controller managed to track the maximum power point under the following conditions:

- Wind speed of 12 m/s.
- Search interval between 350V and 550V
- The voltage step 4V

The output power was very close to the WTG optimal power since it delivers between 6.9 kW and 6.6kW with V_{dc} and I_{dc} values of 438V and15.7A respectively. It is noticed the time taken by this controller to track the MPP is significantly large since it took it 30 seconds to reach it, even though the DC voltage kept oscillating between 432V and 440V without continuously. The efficiency of this algorithm is around 97% and that due to the oscillation between two power values 6.9 kW and 6.6 kW.

4.4.4 Comparative study between GSS and P&O MPPT:

This comparative study is performed for the evaluation of the performance of the proposed GSS MPPT controller and to P&O MPPT controller, in terms of convergence speed, accuracy, and stability (oscillations at the MPP).

Table 4-5: Comparison results.

	Convergence time	Accuracy	Stability
P&O	27 s	97%	300 W
GSS	8.1 s	98%	100 W

The comparison shows that the GSS MPPT algorithm has a much better time response. When it comes to efficiency both algorithms are good and have a high efficiency. Furthermore, the GSS stability is slightly better than the P&O, but a further improvement is required. In sum, the GSS MPPT algorithm in WECS has a better performance than the P&O MPPT algorithm.

GENERAL CONCLUSION

In this project there were three main tasks to achieve. The first task was about designing a variable-speed wind energy conversion system (WECS) driven by permanent magnet synchronous generator (PMSG), the WECS was direct driven (gearless), and the power electronics topology used consisted of uncontrolled three phase rectifier, DC boost converter and two level DC/AC inverter. The second task was the main focus of this project, which was maximum power point tracking based on golden section search (GSS) algorithm applied on machine side to control the input of the boost; thus, control the rotor generator speed. And the last task was synchronizing and connecting the system to the utility grid with minimizing the reactive power transferred between the grid and the system; therefore, assuring a maximum active power transfer from WECS to the grid.

The outcome of this work was mostly achieved, the results obtained from the design of WECS and GSS MPPT were very satisfying, and for the grid connection.
As future work it is intended to add other features to the system, such as yaw control and pitch control, fault detection analysis, and finally redesign the system based on back to back inverter power electronics configuration.

References

1- https://www.researchgate.net/Components-of-Horizontal-Axis-Wind-Turbine_fig1_284395706.

2- US Dept. of Energy – Office of Energy Efficiency and Renewable Energy.

3- http://www.daviddarling.info/encyclopedia/S/AE_swept_area.htm.

4- https://forthewind.weebly.com/design-alternatives.html.

5- Modeling of Load Interfaces for a DriveTrain of a Wind Turbine Master's Thesis in the Master programme Applied Mechanics.

6- L. Zhang, C. Watthansarn and W. Shehered," A matrix converter excited doubly fed Induction machine as a wind power generator," IEEE IECON Conf. Proc., vol. 2, pp 906 - 911, Nov. 2004.

7- PaperEffect of tuned unified power flow controller to mitigate the rotor speed instability of fixed-speed wind turbines.

8- A Tapia, G Tapia, JX Ostolaza and JR Saenz, "WIND ENERGY CONVERSION SYSTEMS GRID CONNECTION," IEEE Transactions on Energy Conversion, Vol.18, pp.194-000.

9- Raju, B. G. Fernandes and Kishore Chatterjee, Department of Electrical Engineering, Indian Institute of Technology Bombay, Powai, Mumbai 400 076, INDIA.

10- Wind turbines, teachergeek.com.

11- Danish Wind Industry Association, http://www.windpower.org/en.

12- Global wind statistics 2016, Global Wind Energy Council.

13- ENERGY HARVESTING Solar, Wind, and Ocean Energy Conversion Systems
Alroza Khaligh Omar G. Onar.

14- A. B "A UPF Power Conditioner with a Simple Maximum Power Point Tracker for Grid Connected Variable Speed Wind Energy Conversion System ".

15- Analysis of the Power Coefficient for a wind generation system. I. Lopez-Garcia G. Espinosa-Pérez Maximiliano Bueno-Lopez.

16- Spera, D.A ed 1994" wind turbine technology: fundamental concept of wind turbine engineering" ASHE press, new York.

17- The 5th International Conference on Electrical Engineering – Boumerdes (ICEE-B) October 29-31, 2017, Boumerdes, Algeria. Intelligent Maximum

Power Tracking Control of PMSG Wind Energy Conversion System. ASRI Aicha, MIHOUB Youcef, HASSAINE Said, ALLAOUI Tayeb.

18- N. Mohan, T. UNDELAND, and W. Robbins 'Power Electronics Converters, Application and Design', New York: John Wiley & Sons, 2003.

19- Power electronics: device, circuit, and application. Muhammad H.RASHID FOURTH EDITION

20- power electronics (lecture note) by Pr. Hamid BENTARZI, institute of electrical and electronic engineering, BOUMERDES, Algeria; 2014/2015

21- Mathematical Modelling of Grid Connected Fixed-Pitch Variable-Speed Permanent Magnet Synchronous Generators for Wind Turbines June 2012.

22- https://www.researchgate.net/Two-mass-system-representing-the-drive-train-of-a-DFIG-wind-turbine_fig1_261224941.

23- https://www.researchgate.net/The-d-q-coordinate-frame-of-the-PMSG_fig9_274919318.

24- https://www.researchgate.net/Equivalent-circuit-of-PMSG-in-a-d-axis-and-b-q-axis_fig1_319258932.

25- Maximum Power Control of Variable Speed Wind Turbine Connected to Permanent Magnet Synchronous Generator Using Chopper Equipped with Superconductive InductorM.B. Bana Sharifian, Y. Mohamadrezapour, M. Hosseinpour and S. Torabzade.

26- http://www.jons-workshop.com/img/3_phase_bridge.png.

27- https://upload.wikimedia.org/wikipedia/commons/e/e9/Boost_converter.svg.

28- https://www.quora.com/Can-all-inverters-DC-to-AC-converter-convert-AC-to-DC-if-used-in-reverse.

29- AALBORG University institute of energy technology vector control of PMSG connected to the grid wind turbine application.

30- Applied Sciences, Volume 7, Issue 4 (April 2017).

31- https://www.researchgate.net/PI-based-control-structure-with-d-q-axis-oriented-cascade-control-of-three-phase-voltage_fig2_224382550.

32- Golden Section Search (GSS) Algorithm for Maximum Power Point Tracking in Photovoltaic System Jaya Agrawal1 ,Mohan Aware2 ,Member IEEE 1,2Electrical Engineering Department 1, 2 Visvesvaraya National Institute of Technology, Nagpur, Indi.

33- Curtis F. Gerald and Patrick O. Wheatley. Applied Numerical Analysis. Seventh Edition, Addison-Wesley, 2004.